Bis(diphenylphosphino)methane-assisted Synthesis of Iron–platinum and –palladium Clusters. Crystal Structures of $[Fe_2Pt(\mu\text{-dppm})(CO)_8]$ and $[FePt_2(\mu\text{-dppm})(CO)_6]$ (dppm = $Ph_2PCH_2PPh_2$) *

Pierre Braunstein and Jean-Luc Richert
Laboratoire de Chimie de Coordination, associé au CNRS (UA 416), Université Louis Pasteur, 4 rue Blaise Pascal, F-67070 Strasbourg Cédex, France
Yves Dusausoy
Laboratoire de Minéralogie et Cristallographie, associé au CNRS (UA 809), Université de Nancy 1, Boîte postale 239, F-54506 Vandoeuvre-les-Nancy Cédex, France

Reactions of $[MCl_2(\text{dppm-}PP')]$ (dppm = $Ph_2PCH_2PPh_2$) complexes with iron carbonyl reagents afforded dppm-bridged Fe–M mixed-metal complexes: $[Fe_2Pt(\mu\text{-dppm})(CO)_8]$ (**1**) was best obtained using $[Fe_2(CO)_9]$, $[FePt_2(\mu\text{-dppm})(CO)_6]$ (**2**) by the reaction with $K[Fe(CO)_3(NO)]$, $[FePt_2(\mu\text{-dppm})_2(CO)_4]$ (**4**) by the reaction with $Na_2[Fe(CO)_4]$, and $[Fe_2Pd(\mu\text{-dppm})_2(CO)_6]$ (**5**) by the reaction with $Na_2[Fe_2(CO)_8]$. Reactions of $[PdM(\mu\text{-dppm})_2Cl_2]$ with $Na_2[Fe(CO)_4]$ afforded $[FeMPd(\mu\text{-dppm})_2(CO)_4]$ (**6**; M = Pd) and (**7**; M = Pt) in high yields. Cluster (**7**) was shown to exist in two isomeric forms. The kinetic isomer, isolated pure at −20 °C, contains a terminal Pd-bound carbonyl whereas the thermodynamic isomer has a terminal Pt-bound carbonyl ligand. A 1:1 ratio is observed at equilibrium. The cluster $[Fe_2Pt(\mu\text{-dppm})_2(CO)_6]$ (**3**) was obtained quantitatively by reaction of (**1**) or $[Fe_2Pt(CO)_9(PPh_3)]$ with 1 or 2 equivalents of dppm. These reactions were shown to occur first by substitution of the Pt-bound carbonyl ligand. Low-yield interconversion of (**1**) and (**2**) was observed as a result of metal-exchange reactions. The structures of clusters (**1**) and (**2**) have been established by single-crystal *X*-ray diffraction studies. In (**1**) a Fe–Pt bond is bridged by the dppm ligand and Fe(1)–Fe(2) 2.740(2), Pt–Fe(1) 2.542(1), and Pt–Fe(2) 2.557(1) Å. In (**2**) the Pt–Pt bond is bridged by the dppm ligand and Fe–Pt(1) 2.541(3), Fe–Pt(2) 2.541(4), and Pt(1)–Pt(2) 2.581(1) Å. The i.r. and n.m.r. spectra (^1H, ^1H-{^{31}P}, and ^{31}P-{^1H}) of the new compounds are reported and discussed.

We have recently reported the synthesis of low-valent, neutral iron–palladium clusters, *e.g.* $[FePd_2(\mu\text{-dppm})_2(CO)_4]$ (**6**) (dppm = $Ph_2PCH_2PPh_2$), and their use as precursors of new heterogeneous, bimetallic catalysts for the selective reductive carbonylation of *o*-nitrophenol to benzoxazol-2-one.[1] Relatively few iron–palladium clusters are known,[2] and we were interested to investigate the use of the redox condensation method for obtaining such clusters. This method would typically involve in this case the reaction of anionic mono- or poly-nuclear iron carbonylates with palladium halogeno complexes.

In the course of these studies we found that many iron–palladium clusters were too unstable to be isolated and/or fully characterized. We therefore decided to investigate the synthesis of iron–platinum clusters which were expected to be more stable and easier to characterize.[3] These would then represent useful structural models for the palladium analogues. We previously demonstrated that the reaction of metal carbonylates with platinum halide complexes is a valuable approach to the synthesis of mixed-metal clusters of various nuclearities.[4] In this paper we present our results concerning the reaction of palladium or platinum halide complexes with $[Fe(CO)_3(NO)]^-$, $[Fe(CO)_4]^{2-}$, $[Fe_2(CO)_8]^{2-}$, and $[Fe_2(CO)_9]$. Preliminary accounts including part of this work have been published.[1a,5]

Results

Reactions of $[PtCl_2(\text{dppm-}PP')]$ *with* $[Fe_2(CO)_9]$, $K[Fe(CO)_3(NO)]$, $Na_2[Fe_2(CO)_8]$, *and* $Na_2[Fe(CO)_4]$. *Characterization of* $[Fe_2Pt(\mu\text{-dppm})(CO)_8]$ (**1**) *and* $[FePt_2(\mu\text{-dppm})(CO)_6]$ (**2**).—The reaction of a large excess of $[Fe_2(CO)_9]$ with $[PtCl_2(\text{dppm-}PP')]$ gave a deep red solution from which $FeCl_2$ was removed by filtration. Purification by column chromatography afforded the following fractions: $[Fe(CO)_5]$, green $[Fe_3(CO)_{12}]$, red $[Fe_2Pt(\mu\text{-dppm})(CO)_8]$ (**1**)[5] (56% yield), orange $[FePt_2(\mu\text{-dppm})(CO)_6]$ (**2**)[5] (6% yield), red $[Fe_2Pt(\mu\text{-dppm})_2(CO)_6]$ (**3**)[5] (traces), and $[FePt_2(\mu\text{-dppm})_2(CO)_4]$ (**4**)[5,6] (8% yield). The last two clusters were generated as a consequence of the column chromatography [Scheme 1, equation (1)] as determined by interpretation of the ^{31}P-{^1H} n.m.r. spectrum of the reaction mixture (see Experimental section).

Monitoring the reaction by ^{31}P-{^1H} n.m.r. spectroscopy indicated some $[PtCl_2(\text{dppm-}PP')]$ (9%) remained after addition (whether stepwise or totally) of 8 equivalents of $[Fe_2(CO)_9]$. The complex $[Fe_2(\mu\text{-dppm})(CO)_7]$[7,8d] and small amounts of unidentified products were also formed. Spectroscopic data given in Tables 1 and 2 are consistent with the structures drawn for (**1**) and (**2**) which were further confirmed by an *X*-ray diffraction study (see below). For complex (**1**), the two protons of the methylene group are equivalent and are coupled to the phosphorus atoms of the dppm ligand with two slightly different coupling constants (10.6 and 12 Hz). This gives rise to a doublet of doublets pattern, with platinum satellites from coupling to ^{195}Pt ($S = \frac{1}{2}$, abundance 33.7%). The ^{31}P-{^1H} n.m.r. spectrum contains

* μ-Bis(diphenylphosphino)methane-2:3κ²*P*,*P*′-octacarbonyl-1κ⁴*C*, 2κ³*C*, 1κ¹*C*-*triangulo*-di-ironplatinum and μ-bis(diphenylphosphino)methane-2:3κ²*P*,*P*′-hexacarbonyl-1κ⁴*C*, 2κ¹*C*, 3κ¹*C*-*triangulo*-irondiplatinum.

Supplementary data available: see Instructions for Authors, *J. Chem. Soc., Dalton Trans.*, 1990, Issue 1, pp. xix—xxii.

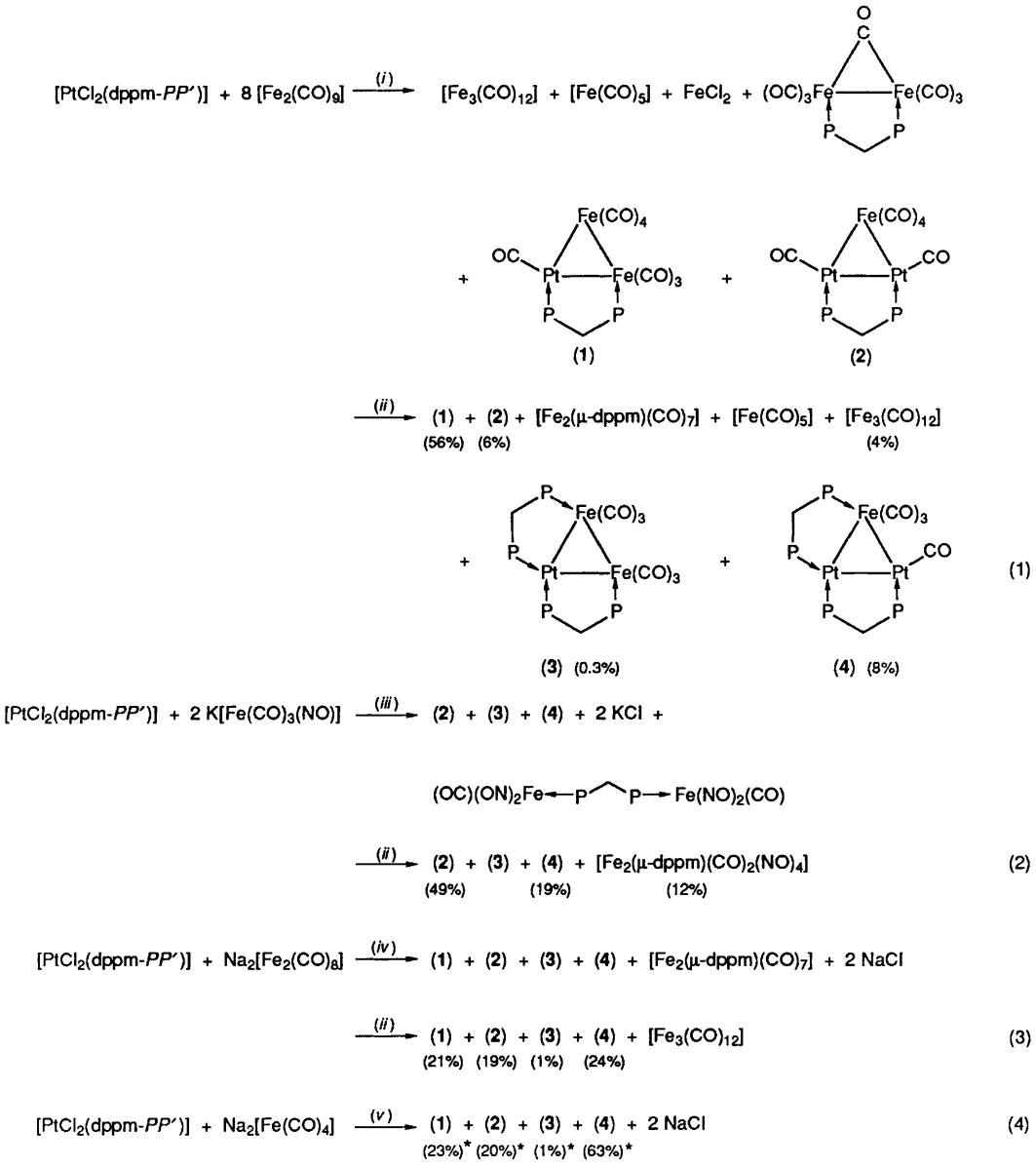

Scheme 1. Isolated yields are based on Pt. (*i*) Tetrahydrofuran (thf), 25 °C, 12 h; (*ii*) chromatography; (*iii*) thf, reflux, 2 h; (*iv*) thf, 0—25 °C, 12 h; (*v*) thf, −20 to 25 °C, 3 h.* ^{31}P N.m.r. spectroscopic yield.

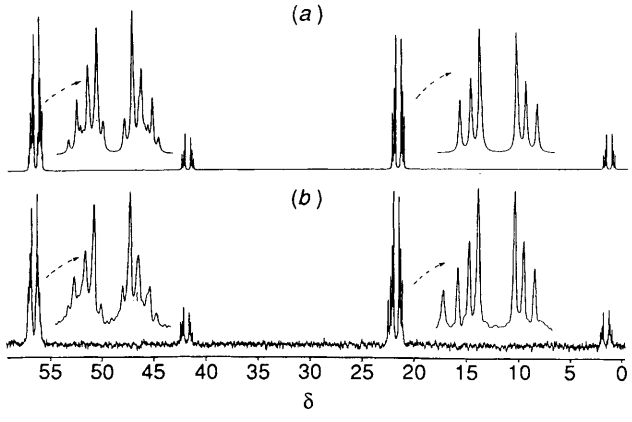

Figure 1. ^{31}P-{^{1}H} n.m.r. spectra of $[Fe_2Pt(\mu\text{-dppm})_2(CO)_6]$ (**3**) (expansion of the signals of the zero-labelled isotopomer in upper traces): (*a*) calculated, (*b*) experimental

two doublets, the high-frequency signal at δ 53.9 being assigned to the phosphorus co-ordinated to iron [8] and the low-frequency one at δ 14.7 with platinum satellites [^{1}J(PtP) = 3 151 Hz] being assigned to P[2].

The ^{1}H n.m.r. signal for the methylene protons of complex (**2**) is typical of a compound containing two Pt atoms [9] and is constituted by the addition of three subspectra. The zero-spin ^{195}Pt isotopomer (abundance 43.95%) gives a triplet [^{2}J(PH) = 11.5 Hz]. Further splitting due to coupling with ^{195}Pt [^{3}J(PtH) = 68 Hz] occurs in the mono and doubly labelled ^{195}Pt isotopomers (abundance 44.68 and 11.35%, respectively). The ^{31}P-{^{1}H} n.m.r. spectrum consists of a singlet at δ −2.4 (A_2 pattern due to the zero-spin ^{195}Pt isotopomer) with satellites characteristic of a symmetrical $Pt_2(\mu\text{-dppm})$ moiety (AA′ parts of the AA′[Pt] and AA′[Pt][Pt′] spin systems of the mono and doubly ^{195}Pt-labelled isotopomers).[10] The ^{31}P-{^{1}H} n.m.r. spectrum of complex (**3**) (Figure 1) consists of two symmetrical signals centred at δ 22 and 57, characteristic of an AA′XX′ spin system, with parameters in the usual range of Pt- and Fe-bound

Table 1. Proton n.m.r. data for the methylene protons of the dppm ligands of complexes (1)—(7)

	Cluster	δ	^2J(PH)/Hz	^4J(PH)/Hz	^3J(PtH)/Hz
(1)[a]	$[Fe_2Pt(\mu\text{-dppm})(CO)_8]$	3.03 (dd)	12.0 P(1)		45.1
			10.6 P(2)		
(2)	$[FePt_2(\mu\text{-dppm})(CO)_6]$	6.14 (t)	11.5		67.9
(3)	$[Fe_2Pt(\mu\text{-dppm})_2(CO)_6]$	4.31 (t)	9.7		37.8
(5)	$[Fe_2Pd(\mu\text{-dppm})_2(CO)_6]$	4.10 (t)	9.7		
(6)	$[FePd_2(\mu\text{-dppm})_2(CO)_4]$	4.42 (dt)	9.8	1.2	
		4.66 (dt)	9.2	2.2	
(7a)[b]	$[FePdPt(\mu\text{-dppm})_2(CO)_4]$	4.66 (ddd)	11.2 P(3)	1.4 P(2)	39.3
			9.6 P(4)		
		5.15 (dt)	9.9 P(1)	2.8 P(3)	57.6
			9.9 P(2)		
(7b)[b]	$[FePdPt(\mu\text{-dppm})_2(CO)_4]$	4.52 (dt)	9.7 P(3)	1.5 P(2)	9[c]
			9.7 P(4)		
		5.27 (ddd)	10.7 P(2)	3 P(3)	63.3
			8.4 P(1)		

[a] The assignments of the coupling constants result from selective proton-decoupling experiments in ^{31}P n.m.r. spectroscopy. [b] The assignments of the coupling constants result from selective phosphorus-decoupling experiments in ^1H n.m.r. spectroscopy. [c] ^4J(PtH).

Table 2. ^{31}P-{^1H} N.m.r. data in thf–C_6D_6

		Chemical shifts (p.p.m.)				Coupling constants J(PP) and J(PtP) in Hz									
	Cluster	P^1	P^2	P^3	P^4	P^1P^2	P^1P^3	P^1P^4	P^2P^3	P^2P^4	P^3P^4	PtP^1	PtP^2	PtP^3	PtP^4
(1)	$[Fe_2Pt(\mu\text{-dppm})(CO)_8]$	53.9	14.7			49						12	3 151		
(2)[a]	$[FePt_2(\mu\text{-dppm})(CO)_6]$	−2.4	−2.4			30						3 187[b]	−74[b]		
(3)[a]	$[Fe_2Pt(\mu\text{-dppm})_2(CO)_6]$	56.6	21.7	21.7	56.6	−60	17	13	0	17	−60	18	3 270	3 270	18
(4)	$[FePt_2(\mu\text{-dppm})_2(CO)_4]$	6.2	7.8	4.3	51.7	44	0	28	2	23	53	3 187[c]	55[c]	130[c]	83[c]
												77[d]	3 480[d]	2 925[d]	24[d]
(5)[a]	$[Fe_2Pd(\mu\text{-dppm})_2(CO)_6]$	55.2	−4.2	−4.2	55.2	−76	18	8	0	18	−76				
(6)[a,e]	$[FePd_2(\mu\text{-dppm})_2(CO)_4]$	−5.3	−7.1	−9.7	52.7	64	0	29	32	28	43				
(7a)[a,f]	$[FePdPt(\mu\text{-dppm})_2(CO)_4]$	−13.5	14.7	4.5	50.7	−55	−12	−36	0	25	−36	−65	3 430	3 264	0
(7b)[e]	$[FePdPt(\mu\text{-dppm})_2(CO)_4]$	15.4	−12.5	−9.2	56	−53	7	−25	26	25	−63	3 213	−43	238	−87
(8)	$[Fe_2Pt(\mu\text{-dppm})(CO)_7(PPh_3)]$	51.7	13.6	38.1		46	17		2			6	3 561	3 208	
(9)	$[Fe_2Pt(\mu\text{-dppm})(CO)_7(PEt_3)]$	55.4	13.3	31.1		48	16		4			21	3 528	3 140	
(10)	$[Fe_2Pt(\mu\text{-dppm})(CO)_6(PEt_3)_2]$	56.9	15.0	29.3	48.3	55	14	3	6	26	3	0	3 186	3 327	14

[a] Coupling constants determined by spectral simulation. [b] Coupling constants of opposite signs, proposed set assuming that ^1J(PtP) is positive; ^1J(PtPt) = 1 373 Hz. [c] $J(Pt^1P)$ coupling constants in the $^{195}Pt(1)$–Pt(2) isotopomer. [d] $J(Pt^2P)$ coupling constants in the Pt(1)–$^{195}Pt(2)$ isotopomer. [e] Errors have been introduced in the labelling of the P atoms in our preliminary communication. [f] Sets of relative signs of the J(PP) and J(PtP) coupling constants (two-dimensional n.m.r. experiment, see text) assuming that $^2J(P^1P^2)$ is negative and ^1J(PtP) positive.

phosphorus nuclei, respectively.[3] The ^{31}P-{^1H} n.m.r. (81 and 162 MHz) spectra of cluster (**4**) could be interpreted in first-order terms and the data are consistent with those reported in the literature.[6]

The reaction of $[PtCl_2(dppm\text{-}PP')]$ with 2 equivalents of $[Fe(CO)_3(NO)]^-$ in thf under reflux afforded the trinuclear clusters (**2**) and (**4**), and the dinuclear iron complex $[Fe_2(\mu\text{-dppm})(CO)_2(NO)_4]$ as major products. In addition, small amounts of (**3**) and unidentified products were also obtained [Scheme 1, equation (2)]. After purification by column chromatography, (**2**) was obtained in 49% yield (based on Pt), (**4**) and $[Fe_2(\mu\text{-dppm})(CO)_2(NO)_4]$ in 19 and 12% yield (based on Pt and dppm, respectively). At present we believe the latter complex has not been described before. It was characterized by ^{31}P n.m.r. and mass spectroscopy and by comparison of its i.r. spectrum with that of the related $[Fe(CO)(NO)_2(PPh_3)]$ complex.[11]

The reaction of $[PtCl_2(dppm\text{-}PP')]$ with 1 equivalent of $Na_2[Fe_2(CO)_8]$ yielded clusters (**1**), (**2**), and (**4**) in a 2:1:2 molar ratio (^{31}P n.m.r. evidence) [Scheme 1, equation (3)]. In addition, each of these clusters was isolated after column chromatography in similar yields, *ca.* 20—30% (based on Pt), thus indicating that transformations on the column had occurred under these conditions. In contrast, the reaction with $Na_2[Fe(CO)_4]$ [Scheme 1, equation (4)] was more selective, affording (**4**) as the major product (*ca.* 60% yield, ^{31}P n.m.r. evidence). Cluster (**4**) has been independently prepared by the reaction of $[Pt_2Cl_2(\mu\text{-dppm})_2]$ with $Na_2[Fe(CO)_4]$.[6]

X-Ray Diffraction Studies of $[Fe_2Pt(\mu\text{-dppm})(CO)_8]$ (**1**) *and* $[FePt_2(\mu\text{-dppm})(CO)_6]$ (**2**).—Views of the molecular structures are shown in Figures 2 and 3 with the atom numbering scheme. Selected bond distances and angles are given in Tables 3 and 4, respectively.

Cluster (**1**) possesses a triangular metallic core with the carbonyl C(8)O(8) in the plane of the three metals. The phosphorus atoms of the dppm ligand bridging the Pt–Fe(1) bond lie above this plane. The platinum atom has a distorted planar geometry and each iron centre could be viewed as in a severely distorted-octahedral environment. The ligands co-ordinated to Fe(1) and Fe(2) are staggered by about 20° whereas they are perfectly staggered in $[Fe_2(CO)_8]^{2-}$.[12] The situation encountered in (**1**) is more similar to that found in the isoelectronic $[FeCo(CO)_8]^-$ anion.[12] A carbonyl ligand on each Fe atom [C(2)O(2) and C(7)O(7)] is semi-bridging[13] the corresponding Pt–Fe bond. The Fe(1)–Fe(2) distance of 2.740(2) Å, although close to the values found in $[Fe_2(CO)_8]^{2-}$ [2.787(2) Å][12] and in the clusters $[Fe_2Pt(CO)_8(PEt_3)_2]$ [2.695(2) Å][3] and $[Fe_2Pt(CO)_9(PPh_3)]$ [2.758(8) Å],[14] is relatively long when compared with the Fe–Fe distances in

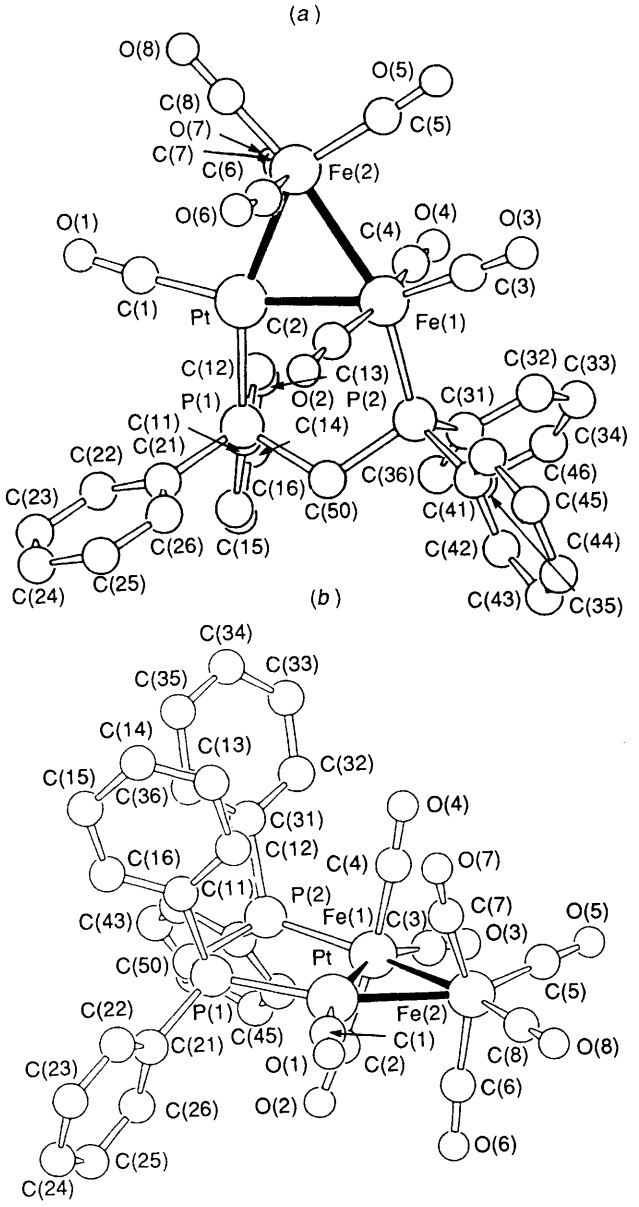

Figure 2. Top (*a*) and perspective (*b*) views of the structure of $[Fe_2Pt(\mu\text{-dppm})(CO)_8]$ (**1**), illustrating the numbering scheme

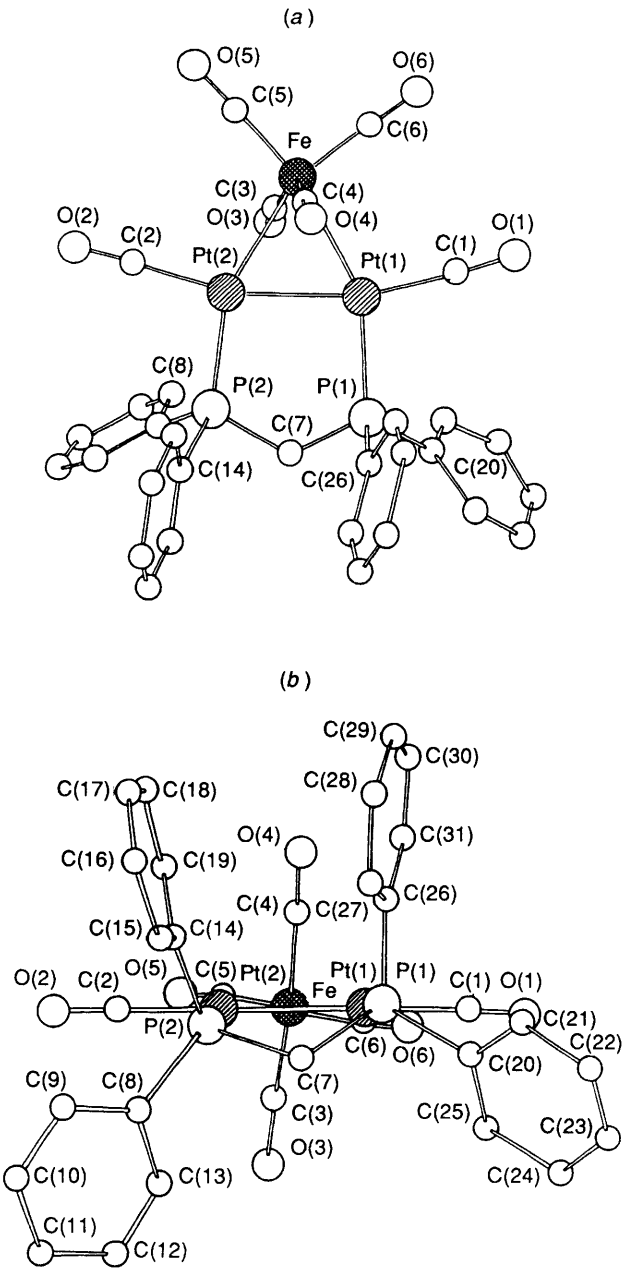

Figure 3. Top (*a*) and perspective (*b*) views of the structure of $[FePt_2(\mu\text{-dppm})(CO)_6]$ (**2**), illustrating the numbering scheme

other mixed iron–platinum clusters (Table 5). The Pt–Fe bond distances are among the shortest reported for Pt–Fe clusters (Table 5). The Pt–Fe(1) bond [2.542(1) Å], bridged by the dppm ligand, is shorter than the Pt–Fe(2) bond [2.557(1) Å]. This could be related to the presence of a CO ligand *trans* to the bond, and a similar effect has been observed in the structure of $[Fe_2Pt(CO)_9(PPh_3)]$.[14]

The isosceles triangular core of complex (**2**) is semi-triply bridged by two CO ligands: C(4)O(4) bridges nearly symmetrically the Pt–Pt bond (the difference between the two Pt–C distances is 0.09 Å), whereas C(3)O(3) is closer to Pt(2) than to Pt(1). The angle between the $FePt_2$ plane and the least-squares plane passing through Fe, C(3), O(3), C(4), and O(4) [maximum deviation 0.03 Å for C(3)] is 97.0°. The co-ordination of the Fe-bound carbonyls is similar to that found in $[Fe_3(CO)_{11}]^{2-}$ (ref. 15) and $[FePt_2(CO)_5\{P(OPh)_3\}_3]$.[16] The phosphorus atoms are each on one side of the plane containing the three metal atoms and the CO ligands co-ordinated to platinum. Neglecting the Fe–Pt bonds, the iron atom has a distorted tetrahedral geometry similar to that in $[Fe(CO)_4]^{2-}$.[17] The Pt–Pt and Fe–Pt bond lengths found in (**2**) are among the shortest reported (see Table 5). In both (**1**) and (**2**), the P–C–P angles [112.4(4) and 108(1)°, respectively] and the M–P–C angles [110.1(3) and 113.3(3), 111.7(7), and 112.2(8)°, respectively] are close to those reported in unidentate dppm complexes, *e.g.* $[Pd(Bu^tNC)_2(dppm\text{-}P)_2]^{2+}$ [111.7(6) and 111.7(3)°],[18] indicating no particular strain in the five-membered ring.

With clusters (**1**) and (**2**) the number of valence electrons (n.v.e.) for iron would be 18 (formal oxidation state −I or −II respectively) and that for platinum would be 16 (formal oxidation state +II or +I, respectively). An alternative bonding description would be to consider three zerovalent metal centres connected by three two-centre two-electron bonds, the 18e iron atom(s) and the 16e platinum atom(s) having their usual n.v.e.

Table 3. Selected bond distances (Å) and angles (°) in $[Fe_2Pt(\mu\text{-dppm})(CO)_8]$ (**1**)

Fe(1)–Fe(2)	2.740(2)	Pt–C(2)	2.65(1)
Pt–Fe(1)	2.542(1)	Pt–C(6)	2.93(1)
Pt–Fe(2)	2.557(1)	Pt–C(7)	2.63(1)
Pt–P(1)	2.262(2)	C(1)–O(1)	1.13(1)
Fe(1)–P(2)	2.208(2)	C(2)–O(2)	1.14(1)
Pt–C(1)	1.88(1)	C(3)–O(3)	1.14(1)
Fe(1)–C(2)	1.78(1)	C(4)–O(4)	1.13(1)
Fe(1)–C(3)	1.77(1)	C(5)–O(5)	1.15(1)
Fe(1)–C(4)	1.79(1)	C(6)–O(6)	1.15(2)
Fe(2)–C(5)	1.79(1)	C(7)–O(7)	1.14(1)
Fe(2)–C(6)	1.77(1)	C(8)–O(8)	1.14(1)
Fe(2)–C(7)	1.77(1)	P(1)–C(50)	1.846(7)
Fe(2)–C(8)	1.76(1)	P(2)–C(50)	1.835(7)
Fe(1)–Fe(2)–Pt	57.2(1)	C(1)–Pt–Fe(1)	165.7(3)
Fe(2)–Fe(1)–Pt	57.8(1)	C(1)–Pt–Fe(2)	100.7(3)
Fe(1)–Pt–Fe(2)	65.0(1)	C(2)–Fe(1)–Pt	73.3(3)
Pt–Fe(1)–P(2)	99.4(1)	C(2)–Fe(1)–Fe(2)	92.2(3)
Fe(1)–Pt–P(1)	93.8(1)	C(3)–Fe(1)–Pt	157.7(4)
Pt–P(1)–C(50)	113.3(3)	C(3)–Fe(1)–Fe(2)	102.8(4)
Fe(1)–P(2)–C(50)	110.1(3)	C(4)–Fe(1)–Pt	91.2(3)
P(1)–C(50)–P(2)	112.4(4)	C(4)–Fe(1)–Fe(2)	81.6(3)
Pt–C(1)–O(1)	176(1)	C(5)–Fe(2)–Fe(1)	88.3(3)
Fe(1)–C(2)–O(2)	174.2(9)	C(5)–Fe(2)–Pt	144.9(3)
Fe(1)–C(3)–O(3)	179(1)	C(6)–Fe(2)–Pt	83.1(4)
Fe(1)–C(4)–O(4)	173(1)	C(6)–Fe(2)–Fe(1)	87.2(4)
Fe(2)–C(5)–O(5)	178(1)	C(7)–Fe(2)–Pt	72.1(3)
Fe(2)–C(6)–O(6)	172(1)	C(7)–Fe(2)–Fe(1)	90.2(3)
Fe(2)–C(7)–O(7)	171.3(9)	C(8)–Fe(2)–Fe(1)	170.7(3)
Fe(2)–C(8)–O(8)	179(1)	C(8)–Fe(2)–Pt	113.6(3)

Reactions of $[PdCl_2(dppm\text{-}PP')]$ *with* $[Fe_2(CO)_9]$, $K[Fe(CO)_3(NO)]$, $Na_2[Fe_2(CO)_8]$, *and* $Na_2[Fe(CO)_4]$.—Of note, $[PdCl_2(dppm\text{-}PP')]$ reacted differently from the platinum analogue. In general, the products could not be isolated pure in the solid state {with the exception of $[Fe_2Pd(\mu\text{-dppm})_2(CO)_6]$ (**5**)}. The ^{31}P n.m.r. spectrum of the reaction mixture indicated that the nature of the products depended strongly on the iron reagent and the stoicheiometry used. With the exception of $[Fe(CO)_4]^{2-}$ where decomposition occurred, products were observed which contained an $Fe(\mu\text{-dppm})_nPd$ ($n = 1$ or 2) moiety (^{31}P n.m.r. evidence, observation of seemingly first-order AA′XX′ patterns).[19] The reaction with $[Fe_2(CO)_8]^{2-}$ [equation (5)] afforded, among others $[Fe_2Pd(\mu\text{-dppm})_2(CO)_6]$ (**5**), which was isolated after precipitation from the reaction mixture and characterized by mass spectroscopy and comparison of its i.r. and ^{31}P-{^1H} n.m.r. data with those of (**3**) (see below).

$$[PdCl_2(dppm\text{-}PP')] + [Fe_2(CO)_8]^{2-} \xrightarrow{\text{thf, } -78 \text{ to } 25\ ^\circ C} \text{(5)}$$

(5)

Reactions of $[PdMCl_2(\mu\text{-dppm})_2]$ (M = Pd *or* Pt) *with* $Na_2[Fe(CO)_4]$.—As a consequence of the formation of clusters (**2**) and (**4**), which contain formally a d^9–d^9 Pt^I–Pt^I bond [equations (1)—(4)], it was expected that the reaction of the d^9–d^9 precursor $[PdMCl_2(\mu\text{-dppm})_2]$ with $Na_2[Fe(CO)_4]$ should lead to triangular clusters of the form $FePdM(\mu\text{-dppm})_2$. Moreover, the reactions (6) and (7) afforded the expected $[FePd_2(\mu\text{-dppm})_2(CO)_4]$ (**6**) and $[FePdPt(\mu\text{-dppm})_2(CO)_4]$ (**7**) in good yields. Details of those reactions have previously been reported.[1a,6]

Table 4. Selected bond distances (Å) and angles (°) in $[FePt_2(\mu\text{-dppm})(CO)_6]$ (**2**)

Fe–Pt(1)	2.541(3)	Fe–Pt(2)	2.541(4)
Pt(1)–Pt(2)	2.581(1)	P(1)–P(2)	2.991(7)
Pt(1)–P(1)	2.252(6)	Pt(2)–P(2)	2.245(6)
Pt(1)–C(1)	1.87(2)	Pt(2)–C(2)	1.87(2)
Pt(1)–C(3)	2.85(3)	Pt(2)–C(3)	2.53(3)
Pt(1)–C(4)	2.64(2)	Pt(2)–C(4)	2.75(2)
Fe–C(3)	1.75(2)	Fe–C(4)	1.80(2)
Fe–C(5)	1.77(2)	Fe–C(6)	1.78(3)
C(1)–O(1)	1.14(3)	C(2)–O(2)	1.14(3)
C(3)–O(3)	1.17(3)	C(4)–O(4)	1.11(2)
C(5)–O(5)	1.15(3)	C(6)–O(6)	1.11(4)
P(1)–C(20)	1.82(2)	P(2)–C(8)	1.81(1)
P(1)–C(26)	1.80(1)	P(2)–C(14)	1.85(2)
P(1)–C(7)	1.84(2)	P(2)–C(7)	1.85(2)
Pt(1)–Pt(2)–Fe	59.48(7)	Pt(1)–Fe–C(6)	96.5(9)
Pt(2)–Pt(1)–Fe	59.47(8)	Pt(2)–Fe–C(3)	69.6(9)
Pt(1)–Fe–Pt(2)	61.09(9)	Pt(2)–Fe–C(4)	76.7(9)
Pt(2)–Pt(1)–P(1)	93.7(1)	Pt(2)–Fe–C(15)	105(1)
Pt(1)–Pt(2)–P(2)	96.3(1)	Pt(2)–Fe–C(6)	156.6(9)
Pt(1)–P(1)–C(7)	111.7(7)	Fe–C(3)–O(3)	175(3)
Pt(2)–P(2)–C(7)	112.2(8)	Fe–C(4)–O(4)	177(2)
P(1)–C(7)–P(2)	108(1)	Fe–C(5)–O(5)	180(2)
Pt(1)–P(1)–C(20)	116(1)	Fe–C(6)–O(6)	177(2)
Pt(1)–P(1)–C(26)	115.4(7)	C(3)–Fe–C(4)	144(1)
Pt(2)–P(2)–C(8)	111.2(7)	C(3)–Fe–C(5)	100.0(9)
Pt(2)–P(2)–C(14)	117.6(7)	C(3)–Fe–C(6)	102(1)
Pt(2)–Pt(1)–C(1)	164.9(6)	C(4)–Fe–C(5)	99(1)
Fe–Pt(1)–C(1)	105.5(7)	C(4)–Fe–C(6)	104(1)
Pt(1)–C(1)–O(1)	176(2)	C(5)–Fe–C(6)	98(1)
Pt(1)–Pt(2)–C(2)	165(1)	C(10)–P(1)–C(7)	101.2(9)
Fe–Pt(2)–C(2)	105(1)	C(26)–P(1)–C(7)	106(1)
Pt(2)–C(2)–O(2)	179(3)	C(20)–P(1)–C(26)	105.7(9)
Pt(1)–Fe–C(3)	81.2(8)	C(7)–P(2)–C(8)	101.7(8)
Pt(1)–Fe–C(4)	72.8(7)	C(7)–P(2)–C(14)	104.7(9)
Pt(1)–Fe–C(5)	165(1)	C(8)–P(2)–C(14)	108.2(9)

It is interesting that the kinetic isomer (**7a**) can be isolated pure at low temperature and that thermal isomerization leads to a 1:1 mixture of (**7a**) and (**7b**) [equation (7)]. Attempts to block the isomerization by substituting the Pd-bound CO by either PhCN, NEt_3, or PMe_2Ph caused decomposition; this may be due to the high reactivity of (**7**) towards CO. When $[PdPt(\mu\text{-dppm})_2Cl_2]$ was treated with $Na_2[Fe_2(CO)_8]$, the species (**3**), (**7a**), and (**7b**) were observed by ^{31}P-{^1H} n.m.r. spectroscopy in a 1:1:1 ratio, whereas $[Pd_2Cl_2(\mu\text{-dppm})_2]$ afforded mainly a homonuclear palladium dppm cluster (**A**) which could not be fully characterized (see below). The reaction of $[Pd_2Cl_2(\mu\text{-dppm})_2]$ with $[Fe_2(CO)_9]$ only led to decomposition and was not further investigated.

Reactivity of Triangular $FePt_2$ *and* Fe_2Pt *Clusters towards Phosphine Ligands.*—These reactions [equations (8)—(14)] were monitored by i.r. spectroscopy and examined by ^{31}P n.m.r. spectroscopy. Selective substitution of the Pt-bound carbonyl ligand of (**1**) with 1 equivalent of tertiary phosphine afforded quantitatively the new clusters $[Fe_2Pt(\mu\text{-dppm})(CO)_7L]$ (**8**; L = PPh_3) and (**9**; L = PEt_3) [Scheme 2, equations (8) and (9)]. Reaction of (**9**) with a second equivalent of PEt_3 in thf at 40 °C produced $[Fe_2Pt(\mu\text{-dppm})(CO)_6(PEt_3)_2]$ (**10**) in *ca.* 50% yield while (**1**) and free PEt_3 were still present [Scheme 2, equation (10)]. It is noteworthy that this reaction with the relatively basic PEt_3 did not go to completion. However, addition of 1 equivalent of dppm to (**1**) afforded cluster (**3**) in high yield, as a result of the entropically favoured five-membered ring formation [Scheme 2, equation (11)]. Similarly,

Table 5. Metal–metal distances (Å) in Fe–Pt complexes

Complex[a]	Distances Fe–Fe	Fe–Pt	Pt–Pt	Ref.
$[FePt(\mu\text{-dppm})(\mu\text{-CO})(CO)_3Br_2]$		2.647(4)		*b,c*
$[FePt(\mu\text{-dppm})(\mu\text{-CO})(CO)_3(PPh_3)]$		2.579(4)		*d,e*
$[FePt(\mu\text{-dppm})\{\mu\text{-C(O)}CH_2C(=CH_2)\}(CO)_3(PPh_3)]$		2.673(4)		*f*
$[FePt(\mu\text{-dppm})\{\mu\text{-C}(=CH_2)CH_2\}(CO)_3(PPh_3)]$		2.634(4)		*e,f*
$[FePt(\mu\text{-dppm})\{\mu\text{-C(O)}C_2H_2\}(CO)_2(PPh_3)]$		2.597(4)		*d,e*
$[FePt(\mu\text{-dppm})(\mu\text{-}\sigma\text{:}\eta^3\text{-CMe=CH}_2)(CO)_3(PPh_3)]^+$		2.630(5)		*d*
$[Fe(CO)_2(\mu\text{-dppm})\{\eta^4\text{-}(CH_2)(CMe_2)CPt(PPh_3)\}]$		2.618(4)		*f*
$[FePt(\mu\text{-dppm})(\mu\text{-I})(CO)_3I]$		2.523(4)		*b,g*
$[FePt(\mu\text{-H})\{\mu\text{-P}(C_6H_{11})_2\}(CO)_3(PEt_3)_2]$		2.800(4)		*h*
$[FePtH(\mu\text{-PPh}_2)(CO)_3(PPh_3)_2]$		2.698(2)		*h*
$[FePt_2(\mu\text{-dppm})(CO)_6]$		2.541(3), 2.541(4)	2.581(1)	This work
$[FePt_2(CO)_5\{P(OPh)_3\}_3]$		2.583(6), 2.550(5)	2.633(1)	16
$[FePt_5(\mu\text{-CO})_4(CO)_5(PEt_3)_4]$		2.603(4)	2.895(1)	*i*
		2.570(4)	2.869(2), 2.767(2),[j] 2.762(2),[j] 2.727(2),[j] 2.722(2), 2.709(1), 2.666(1)[j]	
$[Fe_2Pt(CO)_9(PPh_3)]$	2.758(8)	2.597(5), 2.530(5)		14
$[Fe_2Pt(CO)_8(cod)]$[k]	2.704(4)	2.561(3), 2.553(3)		*l*
$[Fe_2Pt(\mu\text{-dppm})(CO)_8]$	2.740(2)	2.557(1), 2.542(1)		This work
$[Fe_2Pt(\mu\text{-CO})_2(CO)_6(PEt_3)_2]$	2.695(2)	2.640(1), 2.640(1)		3
$[Fe_2Pt(dppe)(CO)_6(\mu\text{-}\eta^2\text{-Bu}^t\text{CP})]$[m]	2.518(1)[n]	2.671(1),[n] 2.669(1)[n]		*o*
$[Fe_2Pt(CO)_6(PhCN)_2]$		2.657(2)		*p*
$[Fe_2Pt_2(\mu\text{-H})_2(CO)_8(PPh_3)_2]$	2.567(4)	2.696(3),[q] 2.694(3),[q] 2.631(3), 2.604(3)	2.998(2)	*l*
$[Fe_2Pt_2(\mu\text{-H})(\mu\text{-CO})_3(CO)_5(PPh_3)_2]^-$	2.522(2)[j]	2.756(2),[q] 2.626(2), 2.562(2),[j] 2.555(2)[j]	2.966(1)	*l*
$[Fe_2Pt_5(\mu\text{-CO})(CO)_{11}(cod)_2]$		2.602(3), 2.591(3), 2.582(3), 2.546(3)	2.958(1),[j] 2.827(1), 2.824(1), 2.802(1), 2.775(1), 2.663(1), 2.643(1), 2.640(1)	*r*
$[Fe_3Pt(\mu_3\text{-H})(\mu_3\text{-COMe})(CO)_{10}(PPh_3)]$	2.556(3),[n] 2.543(2),[n] 2.694(3)[n,q]	2.739(2),[q] 2.696(2),[q] 2.617(2)		*s*
$[Fe_3Pt_3(CO)_{15}]$		2.584(2), 2.580(2), 2.571(1)	2.592(1), 2.592(1), 2.587(2)	*r*
$[Fe_3Pt_3(CO)_{15}]^-$		2.587[t]	2.656[t]	*u*
$[Fe_3Pt_3(CO)_{15}]^{2-}$		2.596[t]	2.750[t]	*u*
$[Fe_4Pt(CO)_{16}]^{2-}$	2.708[t]	2.601[t]		2*a*
$[Fe_4Pt_6(CO)_{22}]^{2-}$		2.597,[t] 2.540[t]	2.790,[t] 2.677[t]	*u*

[a] The complexes are listed with increasing number of Fe atoms and increasing nuclearity. For additional complexes, see: R. D. Adams, I. Arafa, G. Chen, J-C. Lii, and J-G. Wang, *Organometallics*, 1990, **9**, 2350; H. A. Jenkins, S. J. Loeb, D. G. Dick, and D. W. Stephan, *Can. J. Chem.*, 1990, **68**, 869; A. B. Antonova, S. V. Kovalenko, A. A. Ioganson, N. A. Deikhina, E. D. Korniets, Yu. T. Struchkov, Yu. L. Slovokhotov, A. I. Yanovskii, A. G. Ginzburg, and P. V. Petrovskii, *Organomet. Chem. (USSR)*, 1989, **2**, 575. [b] G. B. Jacobsen, B. L. Shaw, and M. Thornton-Pett, *J. Chem. Soc., Dalton Trans.*, 1987, 3079. [c] G. B. Jacobsen, B. L. Shaw, and M. Thornton-Pett, *J. Chem. Soc., Chem. Commun.*, 1986, 13. [d] X. L. R. Fontaine, G. B. Jacobsen, B. L. Shaw, and M. Thornton-Pett, *J. Chem. Soc., Dalton Trans.*, 1988, 741. [e] X. L. R. Fontaine, G. B. Jacobsen, B. L. Shaw, and M. Thornton-Pett, *J. Chem. Soc., Chem. Commun.*, 1987, 662. [f] X. L. R. Fontaine, G. B. Jacobsen, B. L. Shaw, and M. Thornton-Pett, *J. Chem. Soc., Dalton Trans.*, 1988, 1185. [g] G. B. Jacobsen, B. L. Shaw, and M. Thornton-Pett, *Inorg. Chim. Acta*, 1986, 121, L1. [h] J. Powell, M. R. Gregg, and J. F. Sawyer, *J. Chem. Soc., Chem. Commun.*, 1987, 1029. [i] R. Bender, P. Braunstein, D. Bayeul, and Y. Dusausoy, *Inorg. Chem.*, 1989, **28**, 2381. [j] Bridging CO ligand. [k] cod = Cyclo-octa-1,5-diene. [l] L. J. Farrugia, J. A. K. Howard, P. Mitrprachachon, F. G. A. Stone, and P. Woodward, *J. Chem. Soc., Dalton Trans.*, 1981, 1134. [m] dppe = $Ph_2PCH_2CH_2PPh_2$. [n] Other bridging ligands. [o] S. I. Al-Resayes, P. B. Hitchcock, M. F. Meidine, and J. F. Nixon, *J. Chem. Soc., Chem. Commun.*, 1984, 1080. [p] P. Braunstein, G. Predieri, F. J. Lahoz, and A. Tiripicchio, *J. Organomet. Chem.*, 1985, **288**, C13. [q] Bridging H ligand. [r] R. D. Adams, G. Chen, and J. G. Wang, *Polyhedron*, 1989, **8**, 2521. [s] M. Green, K. A. Mead, R. M. Mills, I. D. Salter, F. G. A. Stone, and P. Woodward, *J. Chem. Soc., Chem. Commun.*, 1982, 51. [t] Average value. [u] G. Longoni, M. Manassero, and M. Sansoni, *J. Am. Chem. Soc.*, 1980, **102**, 7973.

cluster (**2**) could be completely converted into the bis(dppm) cluster (**4**) by addition of 1 equivalent of dppm in thf at room temperature [equation (12)]. Further addition of dppm to (**4**) afforded mainly (**11**) [equation (13)].

The 1:1 mixture of compounds (**7a**) and (**7b**) similarly afforded mainly (**12**) [equation (14)]. Monitoring by i.r. spectroscopy at −76 °C during stepwise addition of dppm indicated that (**7a**) reacted slightly faster than (**7b**) (^{31}P n.m.r. monitoring was unsuccessful owing to overlap of the different signals). In contrast, (**3**) did not react, even with a large excess of dppm at 40 °C (Scheme 2), consistent with the observation that substitution of a Pt- or Pd-bound CO ligand in (**1**), (**4**), or (**7**) {disappearance of the strong i.r. ν(CO) absorption at *ca.* 2 050 [(**1**) and (**2**)], 2 024 [(**7a**)], or at *ca.* 2 000 cm^{-1} [(**4**) and (**7b**)]} is easier than that of an Fe-bound CO and represents the first step in the substitution by dppm. The fact that dppm can also displace a Pt-bound monodentate phosphine was shown by the reactions (15) and (16). The former represents a convenient quantitative access to (**3**) more advantageous than that of equation (11), in using the more accessible $[Fe_2Pt(CO)_9(PPh_3)]$.

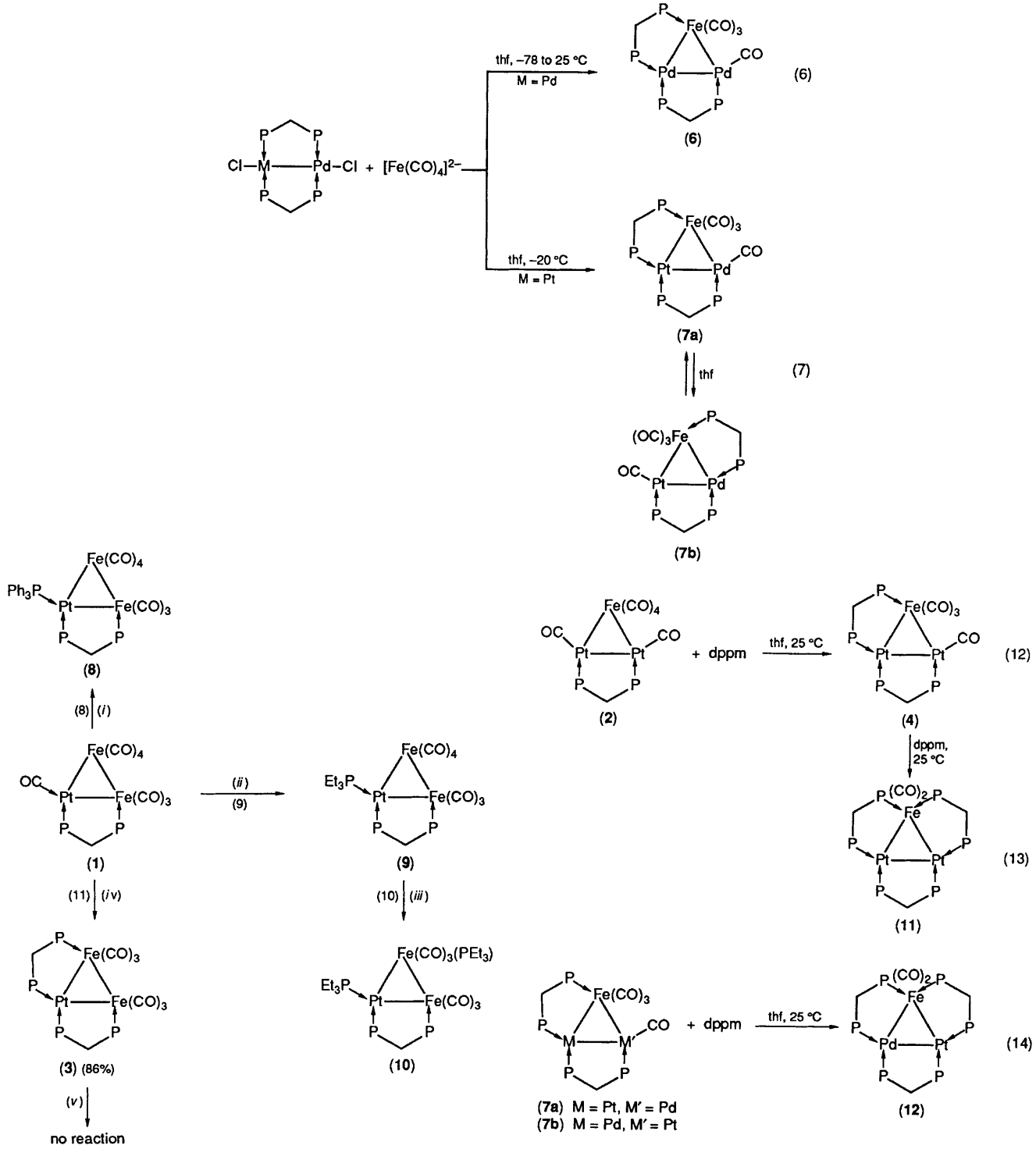

Scheme 2. (*i*) PPh_3, thf, 25 °C; (*ii*) PEt_3, thf, 25 °C; (*iii*) PEt_3, thf, 40 °C; (*iv*) dppm, thf, 25 °C; (*v*) dppm, 40 °C

The structures proposed for compounds (**8**)—(**12**), which were not isolated in the solid state, are based on the interpretation of their ^{31}P n.m.r. spectra. In comparison with (**1**), the spectrum of (**8**) or (**9**) contains a third signal, with ^{195}Pt satellites [$^1J(PtP)$ = 3 208 and 3 140 Hz, respectively], whose chemical shift and coupling constants are in the normal range for a Pt-bound PPh_3 or PEt_3 ligand, respectively.[20] Of note, the addition of the second PEt_3 to (**9**) [producing (**10**)] causes a decrease in $^1J[PtP(2)]$ and an increase in $^1J[PtP(3)]$. With (**10**), the more shielded Fe-bound phosphorus resonance is that of the PEt_3 ligand. Further coupling with this phosphorus atom results in a first-order doublet of doublets of doublets for each nucleus, sometimes unresolved because of small $J(PP)$ values and relatively broad signals (see Table 2). The spectrum of compound (**11**) contains three symmetrical groups of an AA′XX′ZZ′ spin system, the XX′ and ZZ′ parts having ^{195}Pt satellites characteristic of $^1J(PtP)$. The spectrum of (**12**) exhibits six groups of signals with chemical shifts and intensities consistent with the presence of six chemically inequivalent nuclei, two on each metal centre.

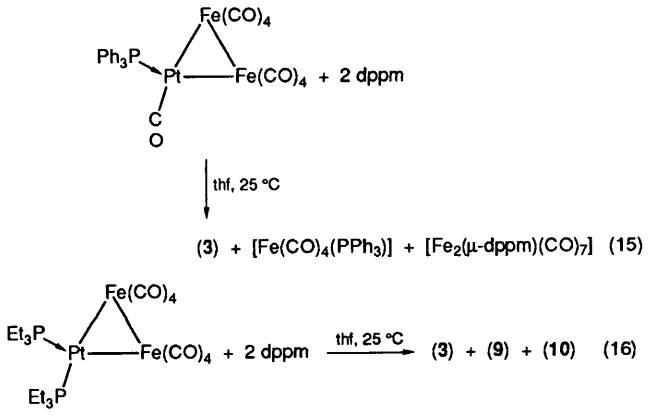

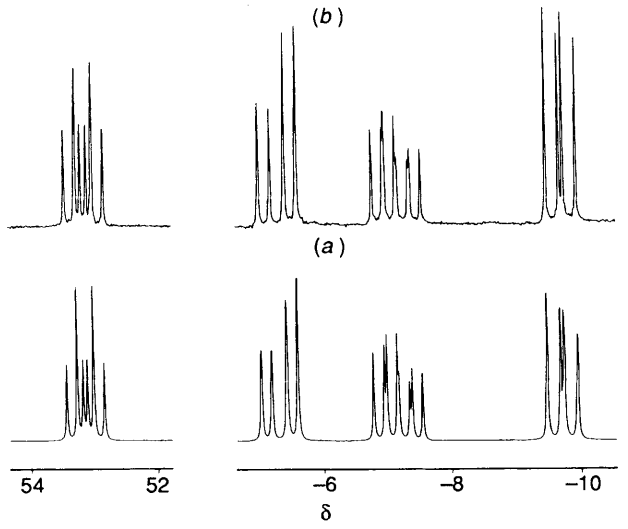

Figure 4. $^{31}P-\{^{1}H\}$ n.m.r. spectra of $[FePd_2(\mu\text{-dppm})_2(CO)_6]$ (**5**): (*a*) calculated, (*b*) experimental

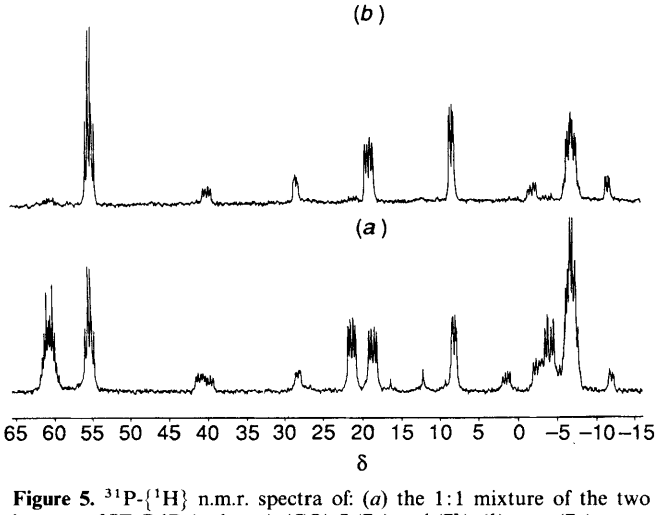

Figure 5. $^{31}P-\{^{1}H\}$ n.m.r. spectra of: (*a*) the 1:1 mixture of the two isomers of $[FePdPt(\mu\text{-dppm})_2(CO)_4]$ (**7a**) and (**7b**); (*b*) pure (**7a**)

Other Reactions of Compounds (**1**), (**2**), *and* (**6**).—The observation of signals attributed to compound (**2**) (M^+ and loss of three CO groups) in the mass spectrum of (**1**) prompted us to investigate their thermal behaviour. Upon refluxing in toluene cluster (**1**) underwent transformation but was not however converted into (**2**). Partial conversion of (**1**) into (**2**) did occur though under CO or upon reaction with $[Fe_2(CO)_9]$ (see Experimental section).

The transformation of compound (**2**) was negligible upon refluxing in toluene where some decomposition occurred and no dppm-containing product was detected. In none of these reactions was free dppm observed. Whereas (**2**) was inert toward CO, it did give a small amount of (**1**) when treated with $[Fe_2(CO)_9]$, also as a result of a metal-exchange reaction (see Experimental section). No higher-nuclearity cluster was observed, in contrast to the reaction of $[Pt_5(CO)_6(PEt_3)_4]$ with $[Fe_2(CO)_9]$ which afforded $[FePt_5(CO)_9(PEt_3)_4]$.[3]

Under CO, compound (**6**) instantaneously and cleanly, and (**7**) more slowly, transformed into $[Fe(dppm\text{-}P)(CO)_4]$ and a palladium dppm homonuclear cluster (**A**), which was also afforded by the reaction of $[Pd(dba)_2]$ (dba = dibenzylideneacetone) with 1 equivalent of dppm under CO (see Experimental section).

Spectroscopic Properties.—Clusters (**3**) and (**6**) exhibit the same i.r. spectra, indicating that the vibrations of the Fe-bound carbonyl ligands are not influenced by the nature of the second metal in these MFe_2 (M = Pd or Pt) cores. The clusters with the core MM′Fe [M = M′ = Pt, (**4**); M = M′ = Pd, (**5**); M = Pd, M′ = Pt, (**7a**) and (**7b**)] possess similar i.r. spectra in the 1 950—1 800 cm^{-1} ν(CO) region, but the frequency of the M- or M′-bound carbonyl ligand depends on the nature of M or M′: changing from Pd to Pt induces a decrease of about 20 cm^{-1}, owing to increased back donation from the more electron-rich platinum *vs.* palladium centre.[21]

From the ^{1}H n.m.r. spectrum, the methylene protons of dppm were always found to be equivalent and generally coupled with three P nuclei in the bis(dppm) clusters, with characteristic $^{2}J(PH)$ values of *ca.* 10 Hz and a third, small $^{4}J(PH)$ of *ca.* 2 Hz.[8d] The splitting gives rise to a doublet of triplets or a doublet of doublets of doublets, depending on the $^{2}J(PH)$ values. It appears that the $^{2}J(PH)$ values are independent of the nature of the metal ligated by the phosphorus atom. Selective decoupling n.m.r. experiments indicated that the more shielded signal of compounds (**7a**) and (**7b**) corresponds to the methylene protons of the dppm ligand bridging the Fe–M (M = Pd or Pt) bond.

The $^{2}J(PP)$ value, which was found to be 120 Hz for free dppm,[22] decreases upon co-ordination {*e.g.* 86 Hz in $[Fe(dppm\text{-}P)(CO)_4]$}. Additionally, when the dppm bridges a metal–metal bond, a decrease in the observed $^{2+3}J(PP)$ coupling constant could be due to opposite signs of the $^{2}J(PP)$ and $^{3}J(PP)$ contributions. The difference observed in $^{2+3}J(PP)$ between compounds (**1**) and (**2**) is mainly the result of the different nature of the metals involved in the $^{3}J(PP)$ coupling constant.

For the bis(dppm) clusters (**4**), (**6**), and (**7**), each phosphorus nucleus is coupled with the other three, producing a first-order pattern (Figures 4 and 5). The n.m.r. spectra of (**7a**) and of the 1:1 mixture of (**7a**) and (**7b**) were carefully studied and an unambiguous assignment resulted from a two-dimensional $[^{31}P–^{31}P]$ correlation spectroscopy (COSY)-45 n.m.r. experiment,[23] which also afforded the relative signs of the coupling constants, and was used for the other bis(dppm) clusters. In general, the values of the chemical shifts were found in the ranges δ P(Fe) 51—56, δ P(Pt) 4—22, and δ P(Pd) −14 to −4. The constants $J(P^1P^2)$ and $J(P^3P^4)$ were found in the range 40—80 Hz, with the exception of the unusually low value for (**2**) (30 Hz). The 'zigzag' coupling constant[24,25] between P^1 and P^3 is smaller than that between P^2 and P^4, which is similar to that found for $[Mo_2(CF_3CO_2)_4(PEt_3)(PBu_3)]$, structurally analogous to $[Mo_2(CF_3CO_2)_4(PBu_3)_2]$ shown by *X*-ray diffraction to have P–Pt–Pt angles of 97.6(1)°.[26] The *cis* $J(P^2P^3)$ coupling was found to be zero when the metal involved is platinum and *ca.* 20 Hz in the case of palladium. Some general trends previously observed for $[MPdFe_2(\mu\text{-dppm})_2(CO)_5(NO)_2]$[24] also apply

here but marked differences were noted, especially concerning $J(P^1P^4)$ and $J(P^3P^4)$ (Table 2).

Discussion

Synthesis of $[Fe_2Pt(\mu\text{-dppm})(CO)_8]$ (**1**) *and* $[FePt_2(\mu\text{-dppm})(CO)_6]$ (**2**).—In reaction (1) the compound $[Fe_2(CO)_9]$ acts as a reducing agent, being partially oxidized to $FeCl_2$ while $[PtCl_2(dppm\text{-}PP')]$ is reduced to give (**1**). Considering the small amount of $[Fe_3(CO)_{12}]$ isolated after chromatography, it is not clear why such a large excess (ten-fold) of $[Fe_2(CO)_9]$ is necessary to drive the reaction to completion. It is noteworthy that (**1**) is isolated in high yield as the major product, in contrast to the reactions involving monodentate phosphines or phosphites which afford *e.g.* $[FePt_2(CO)_5\{P(OPh)_3\}_3]$ and $[Fe_2Pt(CO)_9(PPh_3)]$ in low yields.[27] This illustrates further the assisting role of the dppm ligand in cluster synthesis.

As shown by equation (3), (**1**) is the expected product of a formal substitution of two chlorides in the *cis* position by $[Fe_2(CO)_8]^{2-}$. The reaction is assisted by dppm since the initial four-membered chelate ring transforms into a more stable five-membered ring[5,18,28] by bridging the Pt–Fe(1) bond. As in the other reactions of $[PtCl_2(dppm\text{-}PP')]$ with carbonylmetalates, some metal–metal bond breaking and molecular rearrangements occurred. It is noteworthy that with $K[Fe(CO)_3(NO)]$ no nitrosyl cluster was observed, the only nitrosyl complex formed being $[Fe_2(\mu\text{-dppm})(CO)_2(NO)_4]$.

In contrast, the reactions of $[PdMCl_2(\mu\text{-dppm})_2]$ (M = Pd or Pt) with $[Fe(CO)_4]^{2-}$ afforded the triangular clusters $[FePdM(\mu\text{-dppm})_2(CO)_4]$ in high yields. These clusters were also obtained using $[HFe(CO)_4]^-$ or $[HCrFe(CO)_9]^-$ as an anion.[29]

Carbonyl Substitution by Phosphine Ligands.—It was generally observed that substitution reactions by monodentate phosphines or by dppm occurs first at Pt atoms whereas the Fe-bound carbonyls are difficult or impossible to substitute [Scheme 2, equations (8)—(11)]. Introduction of the dppm ligand by CO substitution in these triangular clusters occurs under mild conditions, in contrast to reactions on *e.g.* Ru_3 clusters,[30] and may be advantageous for obtaining (**3**) from the easily prepared $[Fe_2Pt(CO)_9(PPh_3)]$ [equation (15)]. Formation of clusters containing three dppm ligands, such as (**11**) or (**12**), proceeds first by substitution of the Pt-bound CO ligand, followed by entropically favoured bridge formation. Similar observations have been made for analogous clusters having the core Pd_2Co.[25]

Possible Mechanisms for the Isomerization (**7a**) $\rightleftharpoons$ (**7b**).—We have observed that compound (**7a**) isomerizes cleanly into (**7b**), the position of the 1:1 equilibrium being independent of the temperature, as predicted thermodynamically, but slightly solvent dependent. The mechanism must be intramolecular, without loss of CO, owing to the reactivity of (**7**) towards this reagent. Furthermore, it requires only a low activation energy,[31] since the isomerization occurs at $\geqslant -20$ °C. We propose two possibilities for metal–phosphorus bond cleavage and reformation,[32] both of which could be viewed as concerted CO and phosphorus migrations (Scheme 3).

In (a) the intermediate would result from CO transfer from the Pd to the Fe atom, whereas the Fe-bound phosphorus migrates in the reverse way, in a 'windscreen-wiper like' movement. This intermediate would have an A-frame structure, related to that in $[Pd_2Cl_2(\mu\text{-dppm})_2(\mu\text{-CO})]$[33] by formal 'isolobal substitution' of the μ-CO ligand by its bulky analogue $Fe(CO)_4$. At equilibrium, this intermediate has an equal chance to change into (**7a**) or (**7b**). In (b) the *trans* influence of the Pt–Pd bond[34] would weaken the Pt–P(3) bond, allowing an

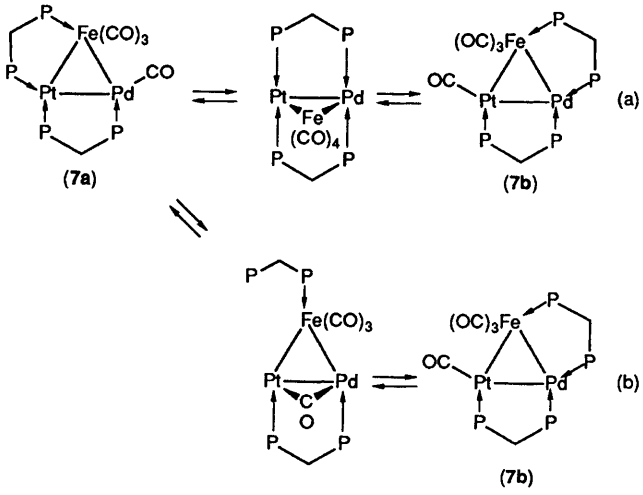

Scheme 3.

easy opening of the five-membered ring and thus generating an intermediate where the unidentate dppm is co-ordinated to the Fe atom while a CO ligand bridges the Pd–Pt bond. Isomerization about the octahedral six-co-ordinated Fe atom would bring the Fe-bound phosphorus transoid to the Pt atom, thus leading to formation of (**7b**). Both mechanisms are consistent with the microreversibility principle. Our ^{31}P n.m.r. experiments unfortunately did not provide reliable information about which phosphorus atoms exchanged positions. High-temperature ^1H and $^{31}P\text{-}\{^1H\}$ n.m.r. spectra showed only slight temperature dependence for some resonances. The rate of isomerization is therefore too slow on the n.m.r. time-scale for successful $^{31}P\text{-}\{^1H\}$ n.m.r. magnetization-transfer experiments.

The reactions described in this paper further demonstrate the potential of dppm as an assembling ligand for the preparation and stabilization of heterometallic complexes. The formation of five-membered rings Fe(μ-dppm)M or M(μ-dppm)M (M = Pd or Pt) constitutes a driving force for these reactions, which is particularly notable when the precursors contain a M(dppm-*PP'*) moiety.

Experimental

Reagents and General Techniques.—General experimental conditions were as previously described.[3,24,25] Silica gel (chromagel, 50—100 mm) was degassed and stored under nitrogen. The compound $[Fe(CO)_5]$ was supplied by BASF; $[Fe_2(CO)_9]$,[35] $Na_2[Fe(CO)_4]$,[36] $Na_2[Fe_2(CO)_8]$,[37] $K[Fe(CO)_3(NO)]$,[38] and $Ph_2PCH_2PPh_2$ (dppm)[39] were prepared according to the literature. The compounds $[PdCl_2(dppm\text{-}PP')]$ and $[PtCl_2(dppm\text{-}PP')]$ were prepared by dropwise addition of a solution of dppm (1 equivalent) to a solution of $[MCl_2(PhCN)_2]$ (M = Pd or Pt) in thf or CH_2Cl_2. The product precipitated in quantitative yield and after filtration was washed with pentane and dried under vacuum. The spectroscopic data are as described in the literature.[40,41] The n.m.r. spectra were recorded on a Bruker WP 200 FT (^1H, 200.13; ^{13}C, 50.32; ^{31}P, 81.02; ^{195}Pt, 42.95 MHz) instrument, unless otherwise specified. The $^1H\text{-}\{^{31}P\}$ n.m.r. spectra were recorded on a Bruker WP 300 FT (^1H, 300 MHz) instrument. ^{31}P N.m.r. spectra were also recorded at 162 MHz on a Bruker AM 400 FT instrument. The ^1H chemical shifts quoted are positive downfield relative to external $SiMe_4$. The chemical shifts of ^{13}C, ^{31}P, and ^{195}Pt n.m.r. spectra are quoted relative to external $SiMe_4$, 85% H_3PO_4 in water, and 0.3 mol dm^{-3} $K_2[PtCl_4]$ in D_2O, respectively, with downfield chemical shifts reported as positive.

The ^1H and ^{31}P-$\{^1H\}$ n.m.r. data are summarized in Tables 1 and 2, respectively. With the seemingly first-order ^{31}P n.m.r. spectra, the notation J' was used to define the apparent coupling constants.

Synthesis of $[Fe_2Pt(\mu\text{-dppm})(CO)_8]$ (**1**).—Tetrahydrofuran (100 cm^3) was added to a solid mixture of $[PtCl_2(dppm\text{-}PP')]\cdot 0.5\ CH_2Cl_2$ (0.67 g, 0.97 mmol) and $[Fe_2(CO)_9]$ (2.84 g, 7.82 mmol). The mixture was stirred overnight, and $FeCl_2$ was removed by filtration. The ^{31}P n.m.r. spectrum of the filtrate contained the signals of (**1**), $[FePt_2(\mu\text{-dppm})(CO)_6]$ (**2**), and $[Fe_2(\mu\text{-dppm})(CO)_7]$ in a *ca.* 26:2:1 molar ratio. The filtrate was concentrated under vacuum to *ca.* 15 cm^3 and adsorbed onto SiO_2, which was added to a chromatography column containing silica gel. Careful elution with CH_2Cl_2–hexane (20:100 v/v) afforded first $[Fe(CO)_5]$,[42] then a green band of $[Fe_3(CO)_{12}]$[43] (0.10 g, 4% yield based on Fe) followed by a red band (35:100 v/v) of (**1**) (0.50 g, 56% yield based on Pt), an orange band (60:100 v/v) of (**2**) (0.03 g, 6% yield based on Pt), a pink-orange band (thf–CH_2Cl_2, 50:50 v/v) containing $[Fe_2Pt(\mu\text{-dppm})_2(CO)_6]$ (**3**) (0.004 g, 0.3% yield based on Pt), and $[FePt_2(\mu\text{-dppm})_2(CO)_4]$ (**4**) (0.04 g, 8% yield based on Pt) as determined by ^{31}P n.m.r. spectroscopy.

$[Fe_2Pt(\mu\text{-dppm})(CO)_8]$ (**1**) (Found: C, 43.40; H, 2.40; Fe, 12.20; P, 6.60; Pt, 21.25. Calc. for $C_{33}H_{22}Fe_2O_8P_2Pt$: C, 43.30; H, 2.40; Fe, 12.20; P, 6.75; Pt, 21.30%); m.p. 197 °C. I.r.: ν(CO) (thf) 2 054s, 2 019s, 1 979s, 1 960s, 1 930w (sh), and 1 908w; (KBr) 2 048s, 2 013s, 1 982s, 1 972s, 1 957s, 1 947s, 1 931s, and 1 888m cm^{-1}. Mass spectrum (chemical ionization, c.i.): *m/z* 915 (M^+), 887 ($M^+ - CO$), 859 ($M^+ - 2CO$), 831 ($M^+ - 3CO$), 801 ($M^+ - 4CO$), 773 ($M^+ - 5CO$), 747 ($M^+ - 6CO$), 719 ($M^+ - 7CO$), and 690 ($M^+ - 8CO$); (electron impact, e.i.) 915 (M^+), 887 ($M^+ - CO$), 859 ($M^+ - 2CO$), and 831 ($M^+ - 3CO$).

Synthesis of $[FePt_2(\mu\text{-dppm})(CO)_6]$ (**2**).—A mixture of $[PtCl_2(dppm\text{-}PP')]\cdot 0.5CH_2Cl_2$ (3.35 g, 4.84 mmol) and $K[Fe(CO)_3(NO)]$ (2.25 g, 10.77 mmol) in thf (175 cm^3) was refluxed for 2.5 h. After a few minutes, the colour changed from yellow to red. The solution was concentrated to a quarter of the volume, filtered, and evaporated to dryness. The solid was dissolved in CH_2Cl_2 (50 cm^3) and adsorbed onto silica gel for column chromatography separation. Elution with CH_2Cl_2–hexane (30:100 v/v) afforded an orange fraction of a new di-iron compound $[\{Fe(CO)(NO)_2\}_2(\mu\text{-dppm})]$ (0.40 g, 12% yield based on dppm; 11% yield based on Fe), then a red band (50:100 v/v) of (**2**) (1.18 g, 49% yield based on Pt), a brownish band (75:100 v/v) containing (**2**), (**3**), $[\{Fe(CO)(NO)_2\}_2(\mu\text{-dppm})]$, and unidentified products, followed by a red band which migrated with difficulty (pure CH_2Cl_2 and finally thf–CH_2Cl_2, 50:50 v/v) of (**4**) (0.60 g, 19% yield based on Pt). Other unidentified products were extracted from the head of the column first with CH_2Cl_2, then acetone: the ^{31}P n.m.r. spectrum of these fractions showed the characteristic pattern of a '$Pt_2(\mu\text{-dppm})_2$' core for one of the products (thf–C_6D_6), δ −12.2 [complex signal with Pt satellites, $^1J(PtP) = 3\,480$, $^2J(PtP) = 170$ Hz].

$[\{Fe(CO)(NO)_2\}_2(\mu\text{-dppm})]$. ^{31}P-$\{^1H\}$ (thf–C_6D_6) δ 43.1s. I.r. (thf): ν(CO) 2 002s; ν(NO) 1 763s and 1 723s cm^{-1}. Mass spectrum (c.i., NH_3): *m/z* 690 ($M + NH_4^+$), 644 ($M - CO$), and 616 ($M - 2CO$).

$[FePt_2(\mu\text{-dppm})(CO)_6]$ (**2**) (Found: C, 37.75; H, 2.10. Calc. for $C_{31}H_{22}FeO_6P_2Pt_2$: C, 37.30; H, 2.20%), m.p. 204 °C. I.r.: ν(CO) (thf) 2 047s, 2 018s, 1 994s, 1 942s, and 1 909s; (KBr) 2 048s, 2 021s, 1 996s, 1 971 (sh), 1 936s, 1 925s, 1 888s, and 1 848 (sh) cm^{-1}. Mass spectrum (c.i.): *m/z* 998 (M^+), 970 ($M^+ - CO$), 942 ($M^+ - 2CO$), 914 ($M^+ - 3CO$), 886 ($M^+ - 4CO$), 858 ($M^+ - 5CO$), and 830 ($M^+ - 6CO$).

$[FePt_2(\mu\text{-dppm})_2(CO)_4]$ (**4**). This cluster has previously been synthesized and i.r. and ^{195}Pt-$\{^1H\}$ data have been reported.[6] Mass spectrum (c.i., CH_4): *m/z* 1 326 (M^+), 1 298 ($M^+ - CO$), 1 270 ($M^+ - 2CO$), 1 242 ($M^+ - 3CO$), and 1 214 ($M^+ - 4CO$).

Synthesis of $[Fe_2Pt(\mu\text{-dppm})_2(CO)_6]$ (**3**).—Cluster (**1**) (0.20 g, 0.22 mmol) and dppm (0.12 g, 0.31 mmol) were dissolved in thf (10 cm^3). The solution was stirred and the colour changed from red to purple-red, the colour of (**3**). After 2 h, the solution was concentrated to half volume, hexane was added, and the mixture was kept for 3 h at −20 °C. The purple-red microcrystals of (**3**) were separated by filtration and dried under vacuum (0.23 g, 0.19 mmol, 86% yield based on Pt). I.r.: ν(CO) (thf) 1 993s, 1 940s, 1 927s, and 1 860w (br); (KBr) 1 986s (br), 1 931s, 1 912s, 1 856w (sh), and 1 840w (br) cm^{-1}. ^{31}P N.m.r. data (Table 2) are typical for a complex containing one Pt atom. Mass spectrum (field desorption, f.d.): *m/z* 1 215 ($M^+ - CO$), 1 103 ($M^+ - 5CO$), and 1 075 ($M^+ - 6CO$).

Reactions of $[PtCl_2(dppm\text{-}PP')]$.—*With* $Na_2[Fe_2(CO)_8]$. Pre-cooled thf (100 cm^3, −76 °C) was added to $[PtCl_2(dppm\text{-}PP')]\cdot 0.5\ CH_2Cl_2$ (0.88 g, 1.27 mmol) and $Na_2[Fe_2(CO)_8]$ (0.59 g, 1.55 mmol). The mixture was stirred and allowed to reach room temperature over 1 h. The solution gradually became deep red and was stirred at room temperature overnight, until all the sparingly soluble $[PtCl_2(dppm\text{-}PP')]$ had disappeared. The ^{31}P n.m.r. spectrum of the reaction mixture contained signals due to compounds (**1**)—(**4**). The solution was evaporated to dryness and the solid residue extracted with toluene. The filtered solution was adsorbed onto silica gel for column chromatography separation. Elution with CH_2Cl_2–hexane (40:100 v/v) afforded a green band of $[Fe_3(CO)_{12}]$, followed by a red band of (**1**) (0.24 g, 21% yield based on Pt), an orange band (60:100 v/v) of (**2**) (0.12 g, 19% yield based on Pt), a brownish band of (**3**) (0.01 g, 1% yield based on Pt), and finally an orange band (pure CH_2Cl_2) of (**4**) (0.20 g, 24% yield based on Pt).

With $Na_2[Fe(CO)_4]$. The reaction was conducted under the same conditions as the preceding reaction, by using $[PtCl_2(dppm\text{-}PP')]$ (0.57 g, 0.82 mmol) and $Na_2[Fe(CO)_4]$ (0.22 g, 1.03 mmol). The ^{31}P n.m.r. spectrum of the toluene extract (0.61 g) produced the following yields based on P: (**1**) (23), (**2**) (20), (**3**) (1), and (**4**) (63%). No other product was detected.

With $[Fe(CO)_5]$. No reaction occurred (^{31}P n.m.r. evidence) when $[PtCl_2(dppm\text{-}PP')]\cdot 0.5CH_2Cl_2$ (0.11 g, 0.16 mmol) and $[Fe(CO)_5]$ (0.15 cm^3, 1.09 mmol) in thf (5 cm^3) were stirred for 3 d in the dark at room temperature.

Synthesis of $[Fe_2Pd(\mu\text{-dppm})_2(CO)_6]$ (**5**).—The compound $[PdCl_2(dppm\text{-}PP')]$ (0.47 g, 0.77 mmol) was treated with $Na_2[Fe_2(CO)_8]$ (0.35 g, 0.92 mmol) in the same manner as previously described for $[PtCl_2(dppm\text{-}PP')]$. The solution became green. The reaction afforded (**5**) and (**B**) which contains an Fe(μ-dppm)Pd moiety (^{31}P-$\{^1H\}$ n.m.r. (thf–C_6D_6) δ 72.1 [d, $J(PP) = 107$, P(Fe)] and 18.0 [d, $J(PP) = 107$ Hz, P(Pd)]). The former precipitated upon addition of hexane (60 cm^3) and cooling the mixture to −20 °C gave a dark green powder (0.22 g, 47% yield based on Pd). Cluster (**5**) was characterized as follows: i.r. ν(CO) (thf) 2 006s, 1 991vs, 1 927s (br), 1 850m, and 1 831 (sh); (KBr) 2 004s, 1 985vs, 1 917br, 1 838m, and 1 832m, cm^{-1}; ^{31}P-$\{^1H\}$ n.m.r. (thf–C_6D_6) (see Table 2); *m/z* (c.i.) 1 155 (M^+). No satisfactory elemental analysis could be obtained for this complex.

Reactions of $[PdCl_2(dppm\text{-}PP')]$ *with* $Na_2[Fe(CO)_4]$ *or* $K[Fe(CO)_3(NO)]$.—A procedure analogous to that for $[PtCl_2(dppm\text{-}PP')]$ was used. With $Na_2[Fe(CO)_4]$, the mixture

changed from grey to green-brown after 1.5 h when room temperature was reached. No mixed Fe–Pd compounds containing dppm were observed by ^{31}P-$\{^1H\}$ n.m.r. study of the solution. With K[$Fe(CO)_3(NO)$] the reaction afforded a yellow-green (−60 °C) to green (0 °C) solution which contained among others compound (**B**).

Reactivity of Compound (**1**) *towards Monodentate Phosphines.*—*With* PPh_3. Pre-cooled thf (10 cm^3, −40 °C) was added to a mixture of compound (**1**) (0.10 g, 0.11 mmol) and 1.15 equivalents of PPh_3 (0.03 g, 0.12 mmol). The colour immediately changed from red to violet-red. The solution was stirred under reduced pressure (to remove CO) until the temperature reached 0 °C. The solution was then degassed every 10 min over the course of an hour at room temperature. The ^{31}P n.m.r. spectrum of the reaction mixture indicated the quantitative formation of [$Fe_2Pt(\mu$-dppm$)(CO)_7(PPh_3)$] (**8**): i.r. ν(CO) (thf) 2 021s, 1 971s, 1 944s, 1 925m (sh), and 1 865w (br) cm^{-1}.

With PEt_3. A solution of compound (**1**) (0.10 g, 0.11 mmol) in thf (7 cm^3) was cooled to −40 °C before addition of 0.18 cm^3 (0.12 mmol) of a solution of PEt_3 [0.5 cm^3 (3.39 mmol) in thf (5 cm^3)]. The reaction was conducted under the above conditions and afforded quantitatively [$Fe_2Pt(\mu$-dppm$)(CO)_7(PEt_3)$] (**9**) (^{31}P n.m.r. evidence): i.r. ν(CO) (thf) 2 020s, 1 964s, 1 941s, and 1 868w (br) cm^{-1}. A second equivalent of PEt_3 was added and the solution was stirred at 30 °C for 5 h; the ^{31}P n.m.r. spectrum of the reaction mixture contained the signals of (**9**) and [$Fe_2Pt(\mu$-dppm$)(CO)_6(PEt_3)_2$] in a *ca.* 1:1 molar ratio.

Substitution of CO *by dppm in* Pt–Fe *Clusters.*—The reaction was conducted under the same conditions as for the synthesis of compound (**3**) (see above), by using (**4**) (0.12 g, 0.09 mmol) and dppm (0.04 g, 0.10 mmol). Cluster (**11**) was identified from the mixture by its ^{31}P n.m.r. spectrum (thf–C_6D_6) which contained three sub-spectra of the types [AA′XX′ZZ′], [AA′XX′ZZ′][Pt], and [AA′XX′ZZ′][Pt][Pt′] which were not fully interpreted: δ 52.6 [m, 2P(Fe)], 11.1 [m, ^1J(PtP) = 3 500, 2P(Pt)], and 5.8 [m, ^1J(PtP) = 3 672 Hz, 2P(Pt)].

The reaction of [$Fe_2Pt(CO)_9(PPh_3)$] (0.03 g, 0.04 mmol) with an excess of dppm (0.04 g, 0.11 mmol) in thf (5 cm^3) afforded compound (**3**) in nearly quantitative spectroscopic yield (^{31}P n.m.r. spectroscopy). Trace amounts of (**4**), [$Fe(CO)_4(PPh_3)$], and [$Fe_2(\mu$-dppm$)(CO)_7$] were also identified.

The cluster [$Fe_2Pt(CO)_8(PEt_3)_2$] (0.136 g, 0.177 mmol) and dppm (0.164 g, 0.428 mmol) were dissolved in thf (5 cm^3) and the mixture stirred at room temperature. The reaction was monitored by i.r. spectroscopy [ν(CO) region] and after 1 d the ^{31}P-$\{^1H\}$ n.m.r. spectrum revealed the presence of compounds (**3**), (**9**), and (**10**).

Thermal Decomposition of Compounds (**1**) *and* (**2**).—Monitoring by ^{31}P-$\{^1H\}$ n.m.r. spectroscopy indicated no transformation of a solution of compound (**1**) in toluene heated in a 10-mm n.m.r. tube at 100 °C for 1 h. A stirred solution of *ca.* 0.10 g of (**1**) or (**2**) in refluxing toluene (3.5 cm^3) for several hours became brown. Thermolysis of (**1**) afforded several new compounds, inspection of which indicated that one of them could be structurally related to (**1**), as shown by the ^{31}P n.m.r. spectrum (thf–C_6D_6): δ 58.5 [d, J(PP) = 48, P(Fe)] and 15.8 [d, J(PP) = 48, ^1J(PtP) = 3 250 Hz P(Pt)]. Cluster (**2**) afforded no pyrolysis products. When the same experiment was repeated for compound (**1**), heating for 24 h produced some decomposition, (**3**), (**4**), and a third unidentified compound as observed by ^{31}P n.m.r. spectroscopy.

Reaction of Compound (**1**) *or* (**2**) *with* [$Fe_2(CO)_9$].—A mixture of compound (**1**) (0.10 g, 0.11 mmol) and [$Fe_2(CO)_9$] (0.54 g, 1.48 mmol) in thf (7.5 cm^3) was stirred for 35 h at room temperature. The solution changed from red to brown to purple-red. The ^{31}P-$\{^1H\}$ n.m.r. spectrum after 0.5, 2, 11, and 35 h indicated that the signals of a new Fe–Pt species {δ 65.6 [d, J(PP) = 82, P(Fe)] and 41.0 [d + dd, J(PP) = 82, ^1J(PtP) = 3 507 Hz, P(Pt)]} increased after 2 h, remained unchanged after 11 h, and then disappeared completely after 35 h. After 1 d, 1.5 cm^3 (*ca.* 0.02 mmol of the starting material) of the mixture was added to [$Fe_2(CO)_9$] (0.23 g, 0.63 mmol) and stirred overnight. It afforded compounds (**1**) and (**4**) in the molar ratio 1:5 (based on ^{31}P-$\{^1H\}$ n.m.r. integration).

Using a similar procedure, compound (**2**) (0.80 g, 0.80 mmol) and [$Fe_2(CO)_9$] (0.84 g, 1.32 mmol) were stirred in thf (7.5 cm^3). The solution turned first brown, then orange-red. The only product which could be detected after 2 h by ^{31}P-$\{^1H\}$ n.m.r. spectroscopy was (**1**) [(**1**) and (**2**) were found in the molar ratio 1:21]. After 35 h, unreacted (**2**) was still present.

Reactions of Compounds (**1**)—(**3**) *and* (**6**) *with* CO.—Complex (**1**) (0.09 g, 0.10 mmol) was dissolved in thf (4 cm^3) and stirred overnight under a CO atmosphere in a Schlenk tube (250 cm^3). The solution changed from red to orange-red. The presence of [$Fe(CO)_5$] was detected by i.r. spectroscopy. A ^{31}P-$\{^1H\}$ n.m.r. study of the solution revealed the signals of (**1**), (**2**), (**4**), and [Fe(dppm-*P*)$(CO)_4$] in a molar ratio of *ca.* 1:3:7.5:1.5.

The same procedure was used for compound (**2**) (0.15 g, 0.15 mmol) which was dissolved in thf (4 cm^3). The solution became darker. No [$Fe(CO)_5$] could be detected by i.r. spectroscopy. The ^{31}P-$\{^1H\}$ n.m.r. spectra after 24 and 48 h indicated unreacted (**2**) and an unidentified complex [δ 35.7s] present in very small amount.

Compound (**3**) was dissolved in thf–C_6D_6 in a 10-mm n.m.r. tube. No modification of the ^{31}P n.m.r. spectrum was observed after CO was bubbled through the solution for 0.1 h and kept under 1.5 atm (*ca.* 1.52 × 10^5 Pa) of CO for 3 h at room temperature.

When CO was bubbled through a solution of compound (**6**) (0.20 g) in thf (30 cm^3) the colour immediately changed from green to brown. The reaction afforded the homonuclear cluster (**A**) and [Fe(dppm-*P*)$(CO)_4$] (^{31}P-$\{^1H\}$ n.m.r. evidence). A large excess of pentane was added to precipitate (**A**). Further purification was achieved by dissolution of (**A**) in CH_2Cl_2 and then precipitation by addition of hexane, cooling to −20 °C, and filtration of the brown precipitate. This was then dried under vacuum (Found: C, 46.0; H, 3.25; P, 8.95; Pd, 35.0%). I.r.: ν(CO) (thf) 1 877s (br), 1 844s (br), and 1 823 (sh); (KBr) 1 982w, 1 920 (sh) (br), 1 874m, 1 842s, and 1 814m cm^{-1}. N.m.r.: ^1H (CD_2Cl_2), δ 3.42 [t, J(PH) = 14]; ^{13}C-$\{^1H\}$ (CD_2Cl_2) δ 229 (s, CO); ^{31}P-$\{^1H\}$ (thf–C_6D_6) δ 11.4 [s, P(Pd)]. Mass spectrum, (e.i.): *m/z* 1 477 and 1 421.

Reaction of [$Fe(CO)_5$] *with Dppm.*—In order to identify by ^{31}P n.m.r. spectroscopy the iron–dppm by-products observed during the syntheses of the mixed-metal clusters, we repeated the reactions by Wegner *et al.*[44] Typically, [$Fe(CO)_5$] (16.59 g, 100 mmol) and dppm (2.8 g, 7.28 mmol) were degassed and dissolved in benzene (60 cm^3). The solution was subjected to u.v. irradiation for 1 d with vigorous stirring. The orange solid [$Fe_2(CO)_9$] (3.01 g) was isolated by filtration and the solution was purified by column chromatography. Elution with toluene–hexane (50:100 v/v) afforded a yellow-green band of [Fe(dppm-*P*)$(CO)_4$] (1.50 g), a yellow band of [Fe(dppm-*PP*′)$(CO)_3$] (0.24 g), an orange band of [$Fe_2(\mu$-dppm$)(CO)_7$] (0.02 g), and a red band of [$Fe_2(\mu$-dppm$)_2(CO)_5$] (0.15 g). These products were identified by comparison of their i.r. data with those in the literature.[8d,44,45] The ^{31}P-$\{^1H\}$ n.m.r. data in thf–C_6D_6 were: [Fe(dppm-*P*)$(CO)_4$], δ 66.3 [d, J(PP) = 86, P(Fe)], and −25.3 [d, J(PP) = 86 Hz]; [8a,c,d] [Fe(dppm-*PP*′)$(CO)_3$], δ 15.0s; [$Fe_2(\mu$-dppm$)(CO)_7$], δ 63.0s; [8d] [$Fe_2(\mu$-dppm$)_2(CO)_5$], δ 68.7s.[8d]

X-*Ray Diffraction Study of* $[Fe_2Pt(\mu\text{-dppm})(CO)_8]$ (**1**).—Red crystals of compound (**1**) were grown from slow diffusion of hexane into a CH_2Cl_2 solution of the complex at −20 °C. A crystal was mounted in a quartz capillary and examined by precession photographs. The crystal was then transferred to an Enraf-Nonius CAD-4 diffractometer and centred in the beam. The cell parameters were determined by a least-squares fit of the setting angles of eight sets of four symmetry-related reflections with $2\theta > 24°$. The collection of data proceeded with monitoring of three reflections every 60 min for control of crystal decay, and with monitoring at the setting angles of three reflections every 100 measured for control of crystal orientation. Neither correction for crystal decay nor for crystal orientation was necessary. Averaging of redundant reflections and rejection of systematically absent reflections yielded 6 270 data which were corrected for Lorentz and polarization effects. An absorption correction was applied, with transmission coefficients ranging from 0.6941 to 0.4132. The structure was solved by the heavy-atom method, and by Fourier difference techniques. All atoms with the exception of the phenyl rings were refined with anisotropic parameters using full-matrix least-squares methods. The phenyl rings were modelled as rigid bodies, with positional parameters of five carbon atoms riding on a pivot atom. Three positional parameters, three rotational parameters, and six isotropic thermal parameters were refined for each phenyl ring. Hydrogen atoms were placed in idealized positions [d(C–H) = 0.96 Å] with an isotropic thermal parameter 1.4 times larger than that of the carbon atoms. An extinction correction was applied: $F' = [1 - (10^{-7}F^2/\sin\theta)]F$. A final difference map showed a highest peak of 1.2 e Å^{-3} at a distance of 0.85 Å from the platinum atom. The SHELX 76 system of programs[46] was employed for structure solution and refinement. The structure converged to the residuals given in Table 6, with $R = \Sigma(||F_o| - |F_c||)/\Sigma|F_o|$ and $R' = [\Sigma w(|F_o| - |F_c|)^2/\Sigma w|F_o|^2]^{\frac{1}{2}}$. The weighting scheme used was $w = 2.0313/[\sigma^2(F) + 0.01F^2]$. Selected distances and angles are given in Table 3, atomic co-ordinates in Table 7 and views of the molecule are shown in Figure 2(*a*) and (*b*).

X-*Ray Diffraction Study of* $[FePt_2(\mu\text{-dppm})(CO)_6]$ (**2**).—Orange crystals suitable for *X*-ray analysis were grown from a CH_2Cl_2–hexane solution at −20 °C. A small sphere (mean diameter = 0.08 mm) was shaped from a larger crystal and used for data collection. Intensity data were collected by the ω—2θ scan method with monochromatized Mo-K_α radiation in the range $3 < \theta < 30°$. Intensities of 6 646 unique reflections were measured, of which 3 770 had $I > 6\sigma(I)$, and were used in the structure solution and refinement. The structure was solved by

Table 6. Summary of crystal data and intensity collection for compounds (**1**) and (**2**)*

Compound	$[Fe_2Pt(dppm)(CO)_8]$ (**1**)	$[FePt_2(dppm)(CO)_6]$ (**2**)
Formula	$C_{33}H_{22}Fe_2O_8P_2Pt$	$C_{31}H_{22}FeO_6P_2Pt_2$
M	915.27	998.49
Space group	$P2_1/n$	$P2_1/c$
a/Å	12.128(1)	13.517(3)
b/Å	12.041(2)	11.326(1)
c/Å	23.697(4)	24.028(6)
β/°	98.9626	59.70(2)
U/Å^3	3 418	3 176
D_c/g cm^{-3}	1.78	2.09
F(000)	1 776	1 872
Crystal size (mm)	0.12 × 0.25 × 0.36	0.08 (mean diameter of sphere)
Diffractometer	Enraf-Nonius CAD-4	Enraf-Nonius CAD-4F
Radiation	Ag-K_α (λ = 0.560 83 Å) Highly oriented graphite mono-chromator	Mo-K_α (λ = 0.709 30 Å)
Temp. (°C)	22	25
μ/cm^{-1}	26.01	98.44
Scan range (°)	0.65 + 0.45 tanθ	1 + 0.35 tanθ
Data collection range (°)	$2 < 2\theta < 42$	$3 < \theta < 30$
No. of unique data	6 270	6 646
Data used	4 824 [$F_o^2 > 2.5\sigma(F_o^2)$]	3 770 [$I > 6\sigma(I)$]
No. of parameters	249	379
R	0.0441	0.059
R'	0.0484	0.066
Largest shift/e.s.d. in final cycle	0.11 [for y of C(22)]	1.54 [for y of C(3)]

* Details in common: monoclinic; $Z = 4$; ω—2θ scans.

Table 7. Atomic fractional co-ordinates for compound (**1**), with estimated standard deviations (e.s.d.s) in parentheses

Atom	x	y	z	Atom	x	y	z
Pt	0.453 1(0)	0.196 1(0)	0.161 3(0)	C(14)	0.627 0(5)	0.635 8(4)	0.123 9(2)
Fe(1)	0.256 8(1)	0.208 3(1)	0.105 3(0)	C(15)	0.586 6(5)	0.657 6(4)	0.174 8(2)
Fe(2)	0.401 1(1)	0.040 7(1)	0.088 5(1)	C(16)	0.531 1(5)	0.574 7(4)	0.200 4(2)
P(1)	0.440 8(2)	0.361 4(2)	0.205 3(1)	C(11)	0.515 9(5)	0.470 1(4)	0.175 2(2)
P(2)	0.209 8(2)	0.374 9(2)	0.132 4(1)	C(22)	0.602 7(5)	0.392 5(6)	0.300 9(3)
C(1)	0.599 7(9)	0.155 4(9)	0.191 6(4)	C(23)	0.643 0(5)	0.389 0(6)	0.359 3(3)
O(1)	0.687 4(7)	0.126 2(9)	0.207 6(4)	C(24)	0.573 5(5)	0.354 3(6)	0.397 6(3)
C(2)	0.243 4(8)	0.158 3(8)	0.174 6(4)	C(25)	0.463 7(5)	0.323 0(6)	0.377 4(3)
O(2)	0.226 7(6)	0.131 5(6)	0.218 6(3)	C(26)	0.423 3(5)	0.326 4(6)	0.319 0(3)
C(3)	0.127 6(9)	0.160 3(9)	0.068 0(4)	C(21)	0.492 8(5)	0.361 2(6)	0.280 7(3)
O(3)	0.045 3(7)	0.127 9(9)	0.043 5(4)	C(32)	0.151 9(5)	0.480 7(4)	0.029 0(2)
C(4)	0.308 9(9)	0.265 5(8)	0.044 7(4)	C(33)	0.152 9(5)	0.565 6(4)	−0.010 9(2)
O(4)	0.332 9(9)	0.308 5(7)	0.006 2(4)	C(34)	0.219 1(5)	0.659 4(4)	0.002 8(2)
C(5)	0.301 5(9)	−0.004 3(8)	0.029 0(4)	C(35)	0.284 4(5)	0.668 3(4)	0.056 5(2)
O(5)	0.239 5(7)	−0.035 9(8)	−0.009 2(4)	C(36)	0.283 5(5)	0.583 5(4)	0.096 5(2)
C(6)	0.357 4(9)	−0.028(1)	0.147 4(5)	C(31)	0.217 2(5)	0.489 7(4)	0.082 8(2)
O(6)	0.339 4(8)	−0.079 9(8)	0.185 5(4)	C(42)	0.036 8(5)	0.505 9(4)	0.160 5(3)
C(7)	0.487 9(9)	0.138 4(8)	0.058 3(4)	C(43)	−0.067 1(5)	0.524 8(4)	0.176 9(3)
O(7)	0.550 5(7)	0.188 8(6)	0.037 5(4)	C(44)	−0.136 0(5)	0.435 3(4)	0.185 1(3)
C(8)	0.507 0(9)	−0.058 5(9)	0.087 7(5)	C(45)	−0.101 0(5)	0.327 0(4)	0.176 9(3)
O(8)	0.576 0(8)	−0.121 8(7)	0.086 1(4)	C(46)	0.002 9(5)	0.308 1(4)	0.160 4(3)
C(12)	0.556 2(5)	0.448 2(4)	0.124 3(2)	C(41)	0.071 8(5)	0.397 6(4)	0.152 2(3)
C(13)	0.611 7(5)	0.531 1(4)	0.098 7(2)	C(50)	0.296 3(6)	0.413 1(7)	0.200 2(3)

Table 8. Atomic fractional co-ordinates for compound (**2**), with e.s.d.s in parentheses

Atom	*x*	*y*	*z*	Atom	*x*	*y*	*z*
Pt(2)	0.848 89(6)	0.231 87(6)	0.122 79(3)	C(11)	1.326(2)	0.345(2)	0.027(1)
Pt(1)	0.700 76(6)	0.397 39(6)	0.147 34(3)	C(12)	1.245(2)	0.396(2)	0.016(1)
Fe	0.716 5(2)	0.222 8(3)	0.076 0(1)	C(13)	1.130(2)	0.381(2)	0.057(1)
P(1)	0.748 4(4)	0.497 9(4)	0.212 0(2)	C(14)	0.911(1)	0.262(2)	0.248(1)
P(2)	0.937 9(4)	0.321 3(4)	0.169 6(2)	C(15)	0.959(2)	0.312(2)	0.279(1)
O(1)	0.522(1)	0.556(2)	0.146 8(8)	C(16)	0.931(2)	0.267(2)	0.341(1)
O(2)	0.993(2)	0.011(2)	0.074(1)	C(17)	0.852(3)	0.184(3)	0.368(1)
O(3)	0.074(1)	0.650(2)	0.014 5(7)	C(18)	0.903(2)	0.134(2)	0.337(1)
O(4)	0.567(1)	0.145(1)	0.208 2(8)	C(19)	0.831(2)	0.176(2)	0.274(1)
O(5)	0.760(2)	−0.008(2)	0.012 1(9)	C(20)	0.737(2)	0.658(2)	0.211(1)
O(6)	0.562(2)	0.316(2)	0.037(1)	C(21)	0.691(2)	0.727(2)	0.266(1)
C(1)	0.587(2)	0.496(2)	0.149 2(8)	C(22)	0.688(3)	0.847(3)	0.263(2)
C(2)	0.938(2)	0.094(2)	0.093(1)	C(23)	0.718(3)	0.894(2)	0.205(2)
C(3)	0.845(2)	0.296(2)	0.023 0(9)	C(24)	0.764(3)	0.835(3)	0.146(2)
C(4)	0.625(2)	0.177(2)	0.158(1)	C(25)	0.775(2)	0.708(2)	0.150(2)
C(5)	0.742(2)	0.083(2)	0.037(1)	C(26)	0.670(1)	0.456(1)	0.295 8(7)
C(6)	0.620(2)	0.278(2)	0.052(1)	C(27)	0.709(2)	0.478(2)	0.336(1)
C(7)	0.902(1)	0.480(2)	0.185(1)	C(28)	0.642(3)	0.446(3)	0.402(1)
C(8)	1.092(1)	0.327(2)	0.115 5(8)	C(29)	0.543(2)	0.393(2)	0.424(1)
C(9)	1.171(2)	0.277(2)	0.128(1)	C(30)	0.501(2)	0.364(2)	0.382(1)
C(10)	1.288(2)	0.288(3)	0.085(1)	C(31)	0.568(2)	0.397(2)	0.319(1)

Patterson and Fourier methods. All atoms were refined anisotropically. The weighting scheme used was $w = 2.098/[\sigma^2(F) + 0.01F^2]$. Convergence of full-matrix least-squares refinement gave a residual of $R = 0.059$. The crystal and data collection parameters are summarized in Table 6. Selected bond distances are given in Table 4, atomic co-ordinates in Table 8, and views of the molecule are shown in Figure 3(*a*) and (*b*).

Additional material available from the Cambridge Crystallographic Data Centre comprises H-atom co-ordinates, thermal parameters, and remaining bond lengths and angles.

Acknowledgements

We thank Atochem for financial support and for a doctoral grant to J-L. R., Johnson-Matthey for a generous loan of $PdCl_2$ and $PtCl_2$, and BASF for a gift of $[Fe(CO)_5]$. We are grateful to Professor H. Vahrenkamp and Dr. R. Planalp (University of Freiburg) for the determination of the crystal structure of $[Fe_2Pt(\mu\text{-dppm})(CO)_8]$ (**1**), to Dr. G. Steinmetz at the Tennessee Eastman Co. (U.S.A.) for obtaining the f.d. mass spectra, and to Dr. T. P. J. Coston for proof-reading the manuscript.

References

1 (*a*) P. Braunstein, J. Kervennal, and J-L. Richert, *Angew. Chem., Int. Ed. Engl.*, 1985, **24**, 768; (*b*) P. Braunstein, R. Devenish, P. Gallezot, B. T. Heaton, C. J. Humphreys, J. Kervennal, S. Mulley, and M. Ries, *ibid.*, 1988, **27**, 927; (*c*) P. Braunstein and J. Rosé, in 'Stereochemistry of Organometallic and Inorganic Compounds,' ed. I. Bernal, Elsevier, Amsterdam, 1989, Vol 3, ch. 1, pp. 3—138.

2 (*a*) G. Longoni, M. Manassero, and M. Sansoni, *J. Am. Chem. Soc.*, 1980, **102**, 3242; (*b*) M. Tachikawa and E. L. Muetterties, *Prog. Inorg. Chem.*, 1981, **28**, 205; (*c*) M. Tachikawa, A. C. Sievert, E. L. Muetterties, M. R. Thompson, C. S. Day, and V. W. Day, *J. Am. Chem. Soc.*, 1980, **102**, 1725.

3 R. Bender, P. Braunstein, J-L. Richert, and Y. Dusausoy, *New. J. Chem.*, 1990, **14**, 569.

4 P. Braunstein, *New. J. Chem.*, 1986, **10**, 365.

5 P. Braunstein, N. Guarino, C. de Méric de Bellefon, and J-L. Richert, *Angew. Chem., Int. Ed. Engl.*, 1987, **26**, 88.

6 M. C. Grossel, R. G. Moulding, and K. R. Seddon, *J. Organomet. Chem.*, 1983, **253**, C50.

7 F. A. Cotton and J. M. Troup, *J. Am. Chem. Soc.*, 1974, **96**, 4422.

8 (*a*) R. L. Keiter, A. L. Rheingold, J. J. Hamerski, and C. K. Castle, *Organometallics*, 1983, **2**, 1635; (*b*) S. G. Davies, J. Hibberd, S. J. Simpson, S. E. Thomas, and O. Watts, *J. Chem. Soc., Dalton Trans.*, 1984, 701; (*c*) G. B. Jacobsen, B. L. Shaw, and M. Thornton-Pett, *ibid.*, 1987, 1509; (*d*) S. Cartwright, J. A. Clucas, R. H. Dawson, D. S. Foster, M. J. Harding, and A. K. Smith, *J. Organomet. Chem.*, 1986, **302**, 403.

9 T. H. Tulip, T. Yamagata, T. Yoshida, R. D. Wilson, J. A. Ibers, and S. Otsuka, *Inorg. Chem.*, 1979, **18**, 2239.

10 R. Bender, P. Braunstein, J-M. Jud, and Y. Dusausoy, *Inorg. Chem.*, 1984, **23**, 4489 and refs. therein.

11 D. W. McBride, S. L. Stafford, and F. G. A. Stone, *Inorg. Chem.*, 1962, **1**, 386.

12 H. B. Chin, M. B. Smith, R. D. Wilson, and R. Bau, *J. Am. Chem. Soc.*, 1974, **96**, 5285.

13 R. H. Crabtree and M. Lavin, *Inorg. Chem.*, 1986, **25**, 805.

14 R. Mason and J. A. Zubieta, *J. Organomet. Chem.*, 1974, **66**, 289; R. Mason, J. A. Zubieta, A. T. T. Hsieh, J. Knight, and M. J. Mays, *Chem. Commun.*, 1971, 200.

15 F. Y-K. Lo, G. Longoni, P. Chini, L. D. Lower, and L. F. Dahl, *J. Am. Chem. Soc.*, 1980, **102**, 7691.

16 V. G. Albano and G. Ciani, *J. Organomet. Chem.*, 1974, **66**, 311; V. G. Albano, G. Ciani, M. I. Bruce, G. Shaw, and F. G. A. Stone, *ibid.*, 1972, **42**, C99.

17 R. G. Teller, R. G. Finke, J. P. Collman, H. B. Chin, and R. Bau, *J. Am. Chem. Soc.*, 1977, **99**, 1104.

18 M. M. Olmstead, C-L. Lee, and A. L. Balch, *Inorg. Chem.*, 1982, **21**, 2712.

19 A. Miedaner and L. DuBois, *Inorg. Chem.*, 1988, **27**, 2479; G. B. Jacobsen and B. L. Shaw, *J. Chem. Soc., Dalton Trans.*, 1987, 2005; S. W. Carr, B. L. Shaw, and M. Thornton-Pett, *J. Chem. Soc., Dalton Trans.*, 1985, 2131; J. A. E. Gibson and M. Cowie, *Organometallics*, 1984, **3**, 722; A. Blagg, A. T. Hutton, P. G. Pringle, and B. L. Shaw, *J. Chem. Soc., Dalton Trans.*, 1984, 1815; B. F. Hoskins, R. J. Stean, and T. W. Turney, *ibid.*, p. 1831; A. T. Hutton, P. G. Pringle, and B. L. Shaw, *Organometallics*, 1983, **2**, 1889.

20 P. S. Pregosin and R. W. Kuntz, '^{31}P and ^{13}C NMR of Transition Metal Phosphine Complexes,' Springer, Berlin, 1979.

21 D. Belli Dell' Amico, F. Calderazzo, C. A. Veracini, and N. Zandonà, *Inorg. Chem.*, 1984, **23**, 3030.

22 I. J. Colquhoun and W. McFarlane, *J. Chem. Soc., Dalton Trans.*, 1982, 1915.

23 J. P. Kintzinger, unpublished work.

24 P. Braunstein, C. de Méric de Bellefon, M. Ries, and J. Fischer, *Organometallics*, 1988, **7**, 332.

25 P. Braunstein, C. de Méric de Bellefon, and M. Ries, *Inorg. Chem.*, 1988, **27**, 1338; 1990, **29**, 1181.

26 D. J. Santurne and A. P. Sattelberger, *Inorg. Chem.*, 1985, **24**, 3477.
27 M. I. Bruce, G. Shaw, and F. G. A. Stone, *J. Chem. Soc., Dalton Trans.*, 1972, 1082.
28 See, for example, C. R. Langrick, D. M. McEwan, P. G. Pringle, and B. L. Shaw, *J. Chem. Soc., Dalton Trans.*, 1983, 2487; C. R. Langrick, P. G. Pringle, and B. L. Shaw, *ibid.*, 1984, 1233; B. R. Lloyd and R. J. Puddephatt, *Inorg. Chim. Acta*, 1984, **90**, L77; S. W. Carr, B. L. Shaw, and M. Thornton-Pett, *J. Chem. Soc., Dalton Trans.*, 1985, 2131; S. Sabo, B. Chaudret, and D. Gervais, *J. Organomet. Chem.*, 1985, **292**, 411; M. C. Grossel, J. R. Batson, R. P. Moulding, and K. R. Seddon, *ibid.*, 1986, **304**, 391; H. B. Laarab, B. Chaudret, F. Dahan, J. Devillers, R. Poilblanc, and S. Sabo-Etienne, *New. J. Chem.*, 1990, **14**, 321 and refs. therein; P. Braunstein, C. de Méric de Bellefon, B. Oswald, and M. Ries, unpublished work.
29 P. Braunstein and B. Oswald, *J. Organomet. Chem.*, 1987, **328**, 229.
30 B. Ambwani, S. Chawla, and A. Poe, *Inorg. Chem.*, 1985, **24**, 2635; G. Lavigne and J. J. Bonnet, *ibid.*, 1981, **20**, 2713; M. I. Bruce, J. G. Matisons, and B. K. Nicholson, *J. Organomet. Chem.*, 1983, **247**, 321.
31 See, for example, F. A. Cotton and G. Wilkinson, 'Advanced Inorganic Chemistry,' 5th edn., Wiley-Interscience, New York, 1988, p. 1325.
32 R. J. Blau and J. H. Espenson, *J. Am. Chem. Soc.*, 1986, **108**, 1962.
33 L. S. Benner and A. L. Balch, *J. Am. Chem. Soc.*, 1978, **100**, 6099.
34 R. J. Blau, J. H. Espenson, S. Kim, and R. A. Jacobson, *Inorg. Chem.*, 1986, **25**, 757; M. Shimura and J. H. Espenson, *ibid.*, 1984, **23**, 4069; T. G. Appleton, H. C. Clark, and L. E. Manzer, *Coord. Chem. Rev.*, 1973, **10**, 335.
35 E. Speyer and H. Wolf, *Ber. Dtsch. Chem. Ges.*, 1927, **60**, 1424.
36 J. P. Collman, R. G. Finke, J. N. Cawse, and J. I. Brauman, *J. Am. Chem. Soc.*, 1977, **99**, 2515.
37 J. P. Collman, R. G. Finke, P. L. Matlock, R. Wahren, R. G. Komoto, and J. I. Brauman, *J. Am. Chem. Soc.*, 1978, **100**, 1119.
38 W. Hieber and H. Beutner, *Z. Anorg. Allg. Chem.*, 1963, **320**, 101.
39 K. Sommer, *Z. Anorg. Allg. Chem.*, 1970, **376**, 37.
40 W. L. Steffen and G. Palenik, *Inorg. Chem.*, 1976, **15**, 2432; F. A. Hartley, *Organomet. Chem. Rev. A*, 1970, **6**, 119; J. R. Doyle, P. E. Slade, and H. B. Jonassen, *Inorg. Synth.*, 1960, **6**, 216; J. M. Jenkins and J. G. Verkade, *ibid.*, 1968, **11**, 108.
41 M. P. Brown, R. J. Puddephatt, M. Rashidi, and K. R. Seddon, *J. Chem. Soc., Dalton Trans.*, 1977, 951.
42 M. Bigorgne, *J. Organomet. Chem.*, 1970, **24**, 211.
43 J. Knight and M. J. Mays, *Chem. Commun.*, 1970, 1006.
44 P. A. Wegner, L. F. Evans, and J. Haddock, *Inorg. Chem.*, 1975, **14**, 192.
45 R. J. Haines, *J. Organomet. Chem.*, 1984, **275**, 99.
46 G. M. Sheldrick, SHELX 76, Crystallographic Programs for Crystal Structure Determination, University of Cambridge, 1976.

Received 9*th July* 1990; *Paper* 0/03060K